“Broadening the knowledge base and supporting the long term professional sustainability of the Research University Centre of Excellence at the University of Szeged by ensuring the rising generation of excellent scientists.

ÚJ SZÉCHENYI TERV

Doctoral School of Mathematics and Computer Science

Stochastic Days in Szeged

26.07.2012.

Exploding solutions of hydrodynamic equations in computer simulations

Carlo Boldrighini

(Sapienza University of Rome)

UNIVERSITAS SCIENTIARUM SZEGEDIENSIS · SZEGEDI TUDOMÁNYEGYETEM ·

TÁMOP-4.2.2/B-10/1-2010-0012 project

MAGYARORSZÁG MEGÚJUL

A projekt az Európai Unió támogatásával, az Európai Szociális Alap társfinanszírozásával valósul meg.

EXPLODING SOLUTIONS
OF HYDRODYNAMIC EQUATIONS
IN COMPUTER SIMULATIONS

EXPLODING SOLUTIONS OF HYDRODYNAMIC EQUATIONS IN COMPUTER SIMULATIONS

C. Boldrighini, Dipartimento di Matematica,
Università di Roma "La Sapienza"

EXPLODING SOLUTIONS OF HYDRODYNAMIC EQUATIONS IN COMPUTER SIMULATIONS

C. Boldrighini, Dipartimento di Matematica,
Università di Roma "La Sapienza"

Based on joint work with S. Frigio, and P. Maponi

EXPLODING SOLUTIONS OF HYDRODYNAMIC EQUATIONS IN COMPUTER SIMULATIONS

C. Boldrighini, Dipartimento di Matematica,
Università di Roma "La Sapienza"

Based on joint work with S. Frigio, and P. Maponi
Università di Camerino

EXPLODING SOLUTIONS OF HYDRODYNAMIC EQUATIONS IN COMPUTER SIMULATIONS

C. Boldrighini, Dipartimento di Matematica,
Università di Roma "La Sapienza"

Based on joint work with S. Frigio, and P. Maponi
Università di Camerino

70th anniversary of Andras Kramli

Szeged, July 26th, 2013

1. INTRODUCTION

1. INTRODUCTION

The question whether the 3-dimensional incompressible Navier-Stokes (NS) equations can become singular at finite times for regular initial data, is one of the main open problems of rigorous fluid mechanics.

1. INTRODUCTION

The question whether the 3-dimensional incompressible Navier-Stokes (NS) equations can become singular at finite times for regular initial data, is one of the main open problems of rigorous fluid mechanics.

Assuming that such singularities exist, how would they appear?

1. INTRODUCTION

The question whether the 3-dimensional incompressible Navier-Stokes (NS) equations can become singular at finite times for regular initial data, is one of the main open problems of rigorous fluid mechanics.

Assuming that such singularities exist, how would they appear?

Could they describe some kind of physical phenomena?

1. INTRODUCTION

The question whether the 3-dimensional incompressible Navier-Stokes (NS) equations can become singular at finite times for regular initial data, is one of the main open problems of rigorous fluid mechanics.

Assuming that such singularities exist, how would they appear?

Could they describe some kind of physical phenomena?

These are relevant questions if we want to address the problem of the NS singularities, either theoretically or by computer evidence.

Leray supposed that such singularities do exist and that they are related to turbulence [Leray 1934].

Leray supposed that such singularities do exist and that they are related to turbulence [Leray 1934].
Modern ideas on turbulence developed independently of the problem of singularities.

Leray supposed that such singularities do exist and that they are related to turbulence [Leray 1934].
Modern ideas on turbulence developed independently of the problem of singularities.

For a long time there was little improvement on the subject.

Leray supposed that such singularities do exist and that they are related to turbulence [Leray 1934].
Modern ideas on turbulence developed independently of the problem of singularities.

For a long time there was little improvement on the subject.
A real breakthrough came only a few years ago, due to the work of Li and Sinai (2003 -).

Leray supposed that such singularities do exist and that they are related to turbulence [Leray 1934].
Modern ideas on turbulence developed independently of the problem of singularities.

For a long time there was little improvement on the subject.
A real breakthrough came only a few years ago, due to the work of Li and Sinai (2003 -).

They gave explicit examples of singularities at finite time for a class of complex-valued solutions of the 3-d NS.

Leray supposed that such singularities do exist and that they are related to turbulence [Leray 1934].
Modern ideas on turbulence developed independently of the problem of singularities.

For a long time there was little improvement on the subject.
A real breakthrough came only a few years ago, due to the work of Li and Sinai (2003 -).

They gave explicit examples of singularities at finite time for a class of complex-valued solutions of the 3-d NS.

Their method also applies to other equations of fluid dynamics, such as the Burgers equations [Li, Sinai 2010].

The singularities appear as a concentration of the energy in a small space region,

The singularities appear as a concentration of the energy in a small space region, as it happens for some physical phenomena (tornadoes).

The singularities appear as a concentration of the energy in a small space region, as it happens for some physical phenomena (tornadoes).

The total energy diverges for the complex-valued solutions.

The singularities appear as a concentration of the energy in a small space region, as it happens for some physical phenomena (tornadoes).

The total energy diverges for the complex-valued solutions.

For real valued solution of the NS equations the energy is bounded by the energy inequality.

The singularities appear as a concentration of the energy in a small space region, as it happens for some physical phenomena (tornadoes).

The total energy diverges for the complex-valued solutions.

For real valued solution of the NS equations the energy is bounded by the energy inequality.

The singular real solutions would show instead a divergence of the enstrophy (the integral of the square of the vorticity).

The singularities appear as a concentration of the energy in a small space region, as it happens for some physical phenomena (tornadoes).

The total energy diverges for the complex-valued solutions.

For real valued solution of the NS equations the energy is bounded by the energy inequality.

The singular real solutions would show instead a divergence of the enstrophy (the integral of the square of the vorticity).

One can expect that they also involve a concentration of the energy in a finite region, and could provide a model of tornado-like phenomena.

A careful analysis of the exploding solutions found by Li and Sinai can provide guidelines for the search of real valued singularities, both by theoretical and computational methods.

A careful analysis of the exploding solutions found by Li and Sinai can provide guidelines for the search of real valued singularities, both by theoretical and computational methods.

I report the results of a study by computer simulations of the complex solutions of the 2-dimensional Burgers equations with no boundary conditions and no external forces.

A careful analysis of the exploding solutions found by Li and Sinai can provide guidelines for the search of real valued singularities, both by theoretical and computational methods.

I report the results of a study by computer simulations of the complex solutions of the 2-dimensional Burgers equations with no boundary conditions and no external forces.

I will also report some recent results on the complex-valued 3-d NS equations.

A careful analysis of the exploding solutions found by Li and Sinai can provide guidelines for the search of real valued singularities, both by theoretical and computational methods.

I report the results of a study by computer simulations of the complex solutions of the 2-dimensional Burgers equations with no boundary conditions and no external forces.

I will also report some recent results on the complex-valued 3-d NS equations.

Why Burgers?

A careful analysis of the exploding solutions found by Li and Sinai can provide guidelines for the search of real valued singularities, both by theoretical and computational methods.

I report the results of a study by computer simulations of the complex solutions of the 2-dimensional Burgers equations with no boundary conditions and no external forces.

I will also report some recent results on the complex-valued 3-d NS equations.

Why Burgers?

It is the simplest model of classical fluid equations for which the esistence of singularities is proved for suitable initial data [Li, Sinai 2010].

2. EXPLODING COMPLEX BURGERS SOLUTIONS

2. EXPLODING COMPLEX BURGERS SOLUTIONS

The Burgers equations for the velocity field $\mathbf{u}(x,t) = (u_1(\mathbf{x},t), u_2(\mathbf{x},t))$ are

2. EXPLODING COMPLEX BURGERS SOLUTIONS

The Burgers equations for the velocity field $\mathbf{u}(x,t) = (u_1(\mathbf{x},t), u_2(\mathbf{x},t))$ are

$$\frac{\partial \mathbf{u}}{\partial t} + \sum_{j=1}^{2} u_j \frac{\partial}{\partial x_j}\mathbf{u} = \Delta \mathbf{u}, \qquad \mathbf{x} = (x_1, x_2) \in \mathbb{R}^2.$$

2. EXPLODING COMPLEX BURGERS SOLUTIONS

The Burgers equations for the velocity field $\mathbf{u}(x,t) = (u_1(\mathbf{x},t), u_2(\mathbf{x},t))$ are

$$\frac{\partial \mathbf{u}}{\partial t} + \sum_{j=1}^{2} u_j \frac{\partial}{\partial x_j} \mathbf{u} = \Delta \mathbf{u}, \qquad \mathbf{x} = (x_1, x_2) \in \mathbb{R}^2.$$

We work with the Fourier transform (multiplied by i) $\mathbf{v}(\mathbf{k},t) = (v_1(\mathbf{k},t), v_2(\mathbf{k},t))$:

2. EXPLODING COMPLEX BURGERS SOLUTIONS

The Burgers equations for the velocity field $\mathbf{u}(x,t) = (u_1(\mathbf{x},t), u_2(\mathbf{x},t))$ are

$$\frac{\partial \mathbf{u}}{\partial t} + \sum_{j=1}^{2} u_j \frac{\partial}{\partial x_j}\mathbf{u} = \Delta \mathbf{u}, \qquad \mathbf{x} = (x_1, x_2) \in \mathbb{R}^2.$$

We work with the Fourier transform (multiplied by i) $\mathbf{v}(\mathbf{k},t) = (v_1(\mathbf{k},t), v_2(\mathbf{k},t))$:

$$\mathbf{v}(\mathbf{k},t) = \frac{i}{2\pi}\int_{\mathbb{R}^2} \mathbf{u}(\mathbf{x},t)e^{i\langle \mathbf{k},\mathbf{x}\rangle}d\mathbf{x}, \qquad \mathbf{k} = (k_1, k_2) \in \mathbb{R}^2$$

$\langle \cdot, \cdot \rangle$ denotes the scalar product in $\mathbb{R}^2$.

2. EXPLODING COMPLEX BURGERS SOLUTIONS

The Burgers equations for the velocity field $\mathbf{u}(x,t) = (u_1(\mathbf{x},t), u_2(\mathbf{x},t))$ are

$$\frac{\partial \mathbf{u}}{\partial t} + \sum_{j=1}^{2} u_j \frac{\partial}{\partial x_j}\mathbf{u} = \Delta \mathbf{u}, \qquad \mathbf{x} = (x_1, x_2) \in \mathbb{R}^2.$$

We work with the Fourier transform (multiplied by i) $\mathbf{v}(\mathbf{k},t) = (v_1(\mathbf{k},t), v_2(\mathbf{k},t))$:

$$\mathbf{v}(\mathbf{k},t) = \frac{i}{2\pi}\int_{\mathbb{R}^2} \mathbf{u}(\mathbf{x},t) e^{i\langle \mathbf{k},\mathbf{x}\rangle} d\mathbf{x}, \qquad \mathbf{k} =(k_1, k_2) \in \mathbb{R}^2$$

$\langle \cdot, \cdot \rangle$ denotes the scalar product in $\mathbb{R}^2$.

$\mathbf{v}$ satisfies the integral equation

$\mathbf{v}$ satisfies the integral equation

$$\mathbf{v}(\mathbf{k},t) = e^{-t\mathbf{k}^2}\mathbf{v}(\mathbf{k},0) +$$
$$+ \int_0^t e^{-(t-s)\mathbf{k}^2} ds \int_{\mathbb{R}^2} \langle \mathbf{v}(\mathbf{k}-\mathbf{k}^{'},s), \mathbf{k}^{'} \rangle \mathbf{v}(\mathbf{k}^{'},s) d\mathbf{k}^{'}, \qquad (1)$$

$\mathbf{v}$ satisfies the integral equation

$$\mathbf{v}(\mathbf{k},t) = e^{-t\mathbf{k}^2}\mathbf{v}(\mathbf{k},0) + \\ + \int_0^t e^{-(t-s)\mathbf{k}^2} ds \int_{\mathbb{R}^2} \langle \mathbf{v}(\mathbf{k}-\mathbf{k}',s), \mathbf{k}' \rangle \mathbf{v}(\mathbf{k}',s) d\mathbf{k}', \qquad (1)$$

with some initial condition $\mathbf{v}(\mathbf{k},0)$.

(As usual $\mathbf{k^2} = k_1^2 + k_2^2$.)

$\mathbf{v}$ satisfies the integral equation

$$\mathbf{v}(\mathbf{k},t) = e^{-t\mathbf{k}^2}\mathbf{v}(\mathbf{k},0) +$$
$$+\int_0^t e^{-(t-s)\mathbf{k}^2} ds \int_{\mathbb{R}^2} \langle \mathbf{v}(\mathbf{k}-\mathbf{k}^{'},s),\mathbf{k}^{'}\rangle \mathbf{v}(\mathbf{k}^{'},s) d\mathbf{k}^{'}, \qquad (1)$$

with some initial condition $\mathbf{v}(\mathbf{k},0)$.

(As usual $\mathbf{k^2} = k_1^2 + k_2^2$.)

We consider real solutions $\mathbf{v}(\mathbf{k},t)$, corresponding to complex solutions in $\mathbf{x}$-space.

$\mathbf{v}$ satisfies the integral equation

$$\mathbf{v}(\mathbf{k},t) = e^{-t\mathbf{k}^2}\mathbf{v}(\mathbf{k},0) +$$
$$+\int_0^t e^{-(t-s)\mathbf{k}^2} ds \int_{\mathbb{R}^2} \langle \mathbf{v}(\mathbf{k}-\mathbf{k}', s), \mathbf{k}' \rangle \mathbf{v}(\mathbf{k}', s) d\mathbf{k}', \qquad (1)$$

with some initial condition $\mathbf{v}(\mathbf{k},0)$.
(As usual $\mathbf{k^2} = k_1^2 + k_2^2$.)

We consider real solutions $\mathbf{v}(\mathbf{k},t)$, corresponding to complex solutions in $\mathbf{x}$-space.

The choice of the initial data for the explosion is done according to the analysis of [Li, Sinai, 2010]:

$\mathbf{v}$ satisfies the integral equation

$$\mathbf{v}(\mathbf{k},t) = e^{-t\mathbf{k}^2}\mathbf{v}(\mathbf{k},0) +$$
$$+ \int_0^t e^{-(t-s)\mathbf{k}^2} ds \int_{\mathbb{R}^2} \langle \mathbf{v}(\mathbf{k}-\mathbf{k}^{'},s), \mathbf{k}^{'} \rangle \mathbf{v}(\mathbf{k}^{'},s) d\mathbf{k}^{'}, \qquad (1)$$

with some initial condition $\mathbf{v}(\mathbf{k},0)$.

(As usual $\mathbf{k^2} = k_1^2 + k_2^2$.)

We consider real solutions $\mathbf{v}(\mathbf{k},t)$, corresponding to complex solutions in $\mathbf{x}$-space.

The choice of the initial data for the explosion is done according to the analysis of [Li, Sinai, 2010]: they are concentrated around a point $\mathbf{k}^{(0)} = (a,a)$, with $a > 0$ large enough:

If $|\mathbf{k}-\mathbf{k}^{(0)}| \leq R$ for some $0 < R < |\mathbf{k}^{(0)}|$, we set

If $|\mathbf{k} - \mathbf{k}^{(0)}| \leq R$ for some $0 < R < |\mathbf{k}^{(0)}|$, we set

$$v_1(\mathbf{k}, 0) = \frac{B}{2\pi\sigma^2} e^{-\frac{(\mathbf{k}-\mathbf{k}^{(0)})^2}{2\sigma^2}} \left(B_1(\mathbf{k}) + \phi^{(1)}(\mathbf{k} - \mathbf{k}^{(0)}) \right) \qquad (2a)$$

$$v_2(\mathbf{k}, 0) = \frac{B}{2\pi\sigma^2} e^{-\frac{(\mathbf{k}-\mathbf{k}^{(0)})^2}{2\sigma^2}} \left(B_2(\mathbf{k}) + \phi^{(2)}(\mathbf{k} - \mathbf{k}^{(0)}) \right) \qquad (2b)$$

If $|\mathbf{k} - \mathbf{k}^{(0)}| \leq R$ for some $0 < R < |\mathbf{k}^{(0)}|$, we set

$$v_1(\mathbf{k}, 0) = \frac{B}{2\pi\sigma^2} e^{-\frac{(\mathbf{k}-\mathbf{k}^{(0)})^2}{2\sigma^2}} \left(B_1(\mathbf{k}) + \phi^{(1)}(\mathbf{k} - \mathbf{k}^{(0)}) \right) \tag{2a}$$

$$v_2(\mathbf{k}, 0) = \frac{B}{2\pi\sigma^2} e^{-\frac{(\mathbf{k}-\mathbf{k}^{(0)})^2}{2\sigma^2}} \left(B_2(\mathbf{k}) + \phi^{(2)}(\mathbf{k} - \mathbf{k}^{(0)}) \right) \tag{2b}$$

and $\mathbf{v}(\mathbf{k}, 0) = 0$ if $|\mathbf{k} - \mathbf{k}^{(0)}| > R$.

If $|\mathbf{k}-\mathbf{k}^{(0)}| \le R$ for some $0 < R < |\mathbf{k}^{(0)}|$, we set

$$v_1(\mathbf{k},0) = \frac{B}{2\pi\sigma^2} e^{-\frac{(\mathbf{k}-\mathbf{k}^{(0)})^2}{2\sigma^2}} \left(B_1(\mathbf{k}) + \phi^{(1)}(\mathbf{k}-\mathbf{k}^{(0)})\right) \qquad (2a)$$

$$v_2(\mathbf{k},0) = \frac{B}{2\pi\sigma^2} e^{-\frac{(\mathbf{k}-\mathbf{k}^{(0)})^2}{2\sigma^2}} \left(B_2(\mathbf{k}) + \phi^{(2)}(\mathbf{k}-\mathbf{k}^{(0)})\right) \qquad (2b)$$

and $\mathbf{v}(\mathbf{k},0) = 0$ if $|\mathbf{k}-\mathbf{k}^{(0)}| > R$.

Here

$$B_1(\mathbf{k}) = 1 + b_0 + (\mathbf{b}^{(1)}, \mathbf{k}-\mathbf{k}^{(0)})$$

$$B_2(\mathbf{k}) = 1 - b_0 + (\mathbf{b}^{(2)}, \mathbf{k}-\mathbf{k}^{(0)}).$$

If $|\mathbf{k}-\mathbf{k}^{(0)}| \leq R$ for some $0 < R < |\mathbf{k}^{(0)}|$, we set

$$v_1(\mathbf{k},0) = \frac{B}{2\pi\sigma^2} e^{-\frac{(\mathbf{k}-\mathbf{k}^{(0)})^2}{2\sigma^2}} \left(B_1(\mathbf{k}) + \phi^{(1)}(\mathbf{k}-\mathbf{k}^{(0)})\right) \tag{2a}$$

$$v_2(\mathbf{k},0) = \frac{B}{2\pi\sigma^2} e^{-\frac{(\mathbf{k}-\mathbf{k}^{(0)})^2}{2\sigma^2}} \left(B_2(\mathbf{k}) + \phi^{(2)}(\mathbf{k}-\mathbf{k}^{(0)})\right) \tag{2b}$$

and $\mathbf{v}(\mathbf{k},0) = 0$ if $|\mathbf{k}-\mathbf{k}^{(0)}| > R$.

Here

$$B_1(\mathbf{k}) = 1 + b_0 + (\mathbf{b}^{(1)}, \mathbf{k}-\mathbf{k}^{(0)})$$

$$B_2(\mathbf{k}) = 1 - b_0 + (\mathbf{b}^{(2)}, \mathbf{k}-\mathbf{k}^{(0)}).$$

$B \in \mathbb{R}_+,\ b_0 \in \mathbb{R},\ \mathbf{b}^{(1)}, \mathbf{b}^{(2)} \in \mathbb{R}^2$, and

$\phi^{(1)}, \phi^{(2)}$ are elements of the Hilbert space $\mathcal{H}$ with norm

$$\|\phi\|^2 = \frac{1}{2\pi\sigma^2} \int_{\mathbb{R}^2} |\phi(\mathbf{k})|^2 e^{-\frac{\mathbf{k}^2}{2\sigma^2}} d^2\mathbf{k} \tag{3}$$

$\phi^{(1)}, \phi^{(2)}$ are elements of the Hilbert space $\mathcal{H}$ with norm

$$\|\phi\|^2 = \frac{1}{2\pi\sigma^2} \int_{\mathbb{R}^2} |\phi(\mathbf{k})|^2 e^{-\frac{\mathbf{k}^2}{2\sigma^2}} d^2\mathbf{k} \tag{3}$$

and are orthogonal to the constants and to the linear functions $k_1 - a,\ k_2 - a$.

$\phi^{(1)}, \phi^{(2)}$ are elements of the Hilbert space $\mathcal{H}$ with norm

$$\|\phi\|^2 = \frac{1}{2\pi\sigma^2} \int_{\mathbb{R}^2} |\phi(\mathbf{k})|^2 e^{-\frac{\mathbf{k}^2}{2\sigma^2}} d^2\mathbf{k} \tag{3}$$

and are orthogonal to the constants and to the linear functions $k_1 - a,\ k_2 - a$.

For σ, a and $\phi^{(1)}, \phi^{(2)}$ fixed, the equations (2a,b) define a 6-parameter family of initial conditions.

$\phi^{(1)}, \phi^{(2)}$ are elements of the Hilbert space $\mathcal{H}$ with norm

$$\|\phi\|^2 = \frac{1}{2\pi\sigma^2} \int_{\mathbb{R}^2} |\phi(\mathbf{k})|^2 e^{-\frac{\mathbf{k}^2}{2\sigma^2}} d^2\mathbf{k} \tag{3}$$

and are orthogonal to the constants and to the linear functions $k_1 - a$, $k_2 - a$.

For σ, a and $\phi^{(1)}, \phi^{(2)}$ fixed, the equations (2a,b) define a 6-parameter family of initial conditions.

The parameters are B and $\mathbf{b} = (b_0, \mathbf{b}^{(1)}, \mathbf{b}^{(2)})$:

$\phi^{(1)}, \phi^{(2)}$ are elements of the Hilbert space $\mathcal{H}$ with norm

$$\|\phi\|^2 = \frac{1}{2\pi\sigma^2} \int_{\mathbb{R}^2} |\phi(\mathbf{k})|^2 e^{-\frac{\mathbf{k}^2}{2\sigma^2}} d^2\mathbf{k} \tag{3}$$

and are orthogonal to the constants and to the linear functions $k_1 - a,\ k_2 - a$.

For σ, a and $\phi^{(1)}, \phi^{(2)}$ fixed, the equations (2a,b) define a 6-parameter family of initial conditions.

The parameters are B and $\mathbf{b} = (b_0, \mathbf{b}^{(1)}, \mathbf{b}^{(2)})$:
$\mathbf{b}^{(i)} = (b_1^{(i)}, b_2^{(i)}),\ i = 1, 2.$

$\phi^{(1)}, \phi^{(2)}$ are elements of the Hilbert space $\mathcal{H}$ with norm

$$\|\phi\|^2 = \frac{1}{2\pi\sigma^2} \int_{\mathbb{R}^2} |\phi(\mathbf{k})|^2 e^{-\frac{\mathbf{k}^2}{2\sigma^2}} d^2\mathbf{k} \tag{3}$$

and are orthogonal to the constants and to the linear functions $k_1 - a,\ k_2 - a$.

For σ, a and $\phi^{(1)}, \phi^{(2)}$ fixed, the equations (2a,b) define a 6-parameter family of initial conditions.

The parameters are B and $\mathbf{b} = (b_0, \mathbf{b}^{(1)}, \mathbf{b}^{(2)})$:
$\mathbf{b}^{(i)} = (b_1^{(i)}, b_2^{(i)}),\ i = 1, 2.$

For $\mathbf{b}$ we use the norm $\|\mathbf{b}\| := \max\{|b_0|, |b_j^{(i)}|, i, j = 1, 2\}.$

The following theorem is proved in [Li, Sinai, 2010].

The following theorem is proved in [Li, Sinai, 2010].

Theorem. *For any family of initial data (2a,b), one can find* $\rho_0 > 0$*, a time interval* $\mathcal{J} = [\tau_1, \tau_2]$*,* $0 < \tau_1 < \tau_2$ *and functions* $B(\tau)$*, and* $\mathbf{b}(\tau)$ *on* $\mathcal{J}$*, with* $\|\mathbf{b}(\tau)\| \le \rho_0$*, such that the solution of the Burgers equations with initial data specified by* $B(\tau), \mathbf{b}(\tau)$*,* $\tau \in \mathcal{J}$*, develop a singularity of the energy at* $t = \tau$*.*

The following theorem is proved in [Li, Sinai, 2010].

Theorem. *For any family of initial data (2a,b), one can find* $\rho_0 > 0$*, a time interval* $\mathcal{J} = [\tau_1, \tau_2]$*,* $0 < \tau_1 < \tau_2$ *and functions* $B(\tau)$*, and* $\mathbf{b}(\tau)$ *on* $\mathcal{J}$*, with* $\|\mathbf{b}(\tau)\| \leq \rho_0$*, such that the solution of the Burgers equations with initial data specified by* $B(\tau), \mathbf{b}(\tau)$*,* $\tau \in \mathcal{J}$*, develop a singularity of the energy at* $t = \tau$*.*

A sketch of the proof is necessary to understand the nature and the behavior of the singularities.

The following theorem is proved in [Li, Sinai, 2010].

Theorem. *For any family of initial data (2a,b), one can find* $\rho_0 > 0$*, a time interval* $\mathcal{J} = [\tau_1, \tau_2]$*,* $0 < \tau_1 < \tau_2$ *and functions* $B(\tau)$*, and* $\mathbf{b}(\tau)$ *on* $\mathcal{J}$*, with* $\|\mathbf{b}(\tau)\| \leq \rho_0$*, such that the solution of the Burgers equations with initial data specified by* $B(\tau), \mathbf{b}(\tau)$*,* $\tau \in \mathcal{J}$*, develop a singularity of the energy at* $t = \tau$*.*

A sketch of the proof is necessary to understand the nature and the behavior of the singularities.

The proof is based on a variant of the renormalization group method.

The following theorem is proved in [Li, Sinai, 2010].

Theorem. *For any family of initial data (2a,b), one can find $\rho_0 > 0$, a time interval $\mathcal{J} = [\tau_1, \tau_2]$, $0 < \tau_1 < \tau_2$ and functions $B(\tau)$, and $\mathbf{b}(\tau)$ on $\mathcal{J}$, with $\|\mathbf{b}(\tau)\| \leq \rho_0$, such that the solution of the Burgers equations with initial data specified by $B(\tau), \mathbf{b}(\tau)$, $\tau \in \mathcal{J}$, develop a singularity of the energy at $t = \tau$.*

A sketch of the proof is necessary to understand the nature and the behavior of the singularities.

The proof is based on a variant of the renormalization group method.

Write the initial data as $\mathbf{w}^{(A)}(\mathbf{k}) = A\mathbf{w}^{(1)}(\mathbf{k})$, where A is a parameter, and $\mathbf{w}^{(1)}$ is a function of the type (2a,b).

The solution of the Burgers equation is written as a series

The solution of the Burgers equation is written as a series

$$\mathbf{w}^{(A)}(\mathbf{k},t) = A\, e^{-t\mathbf{k}^2}\mathbf{w}^{(1)}(\mathbf{k}) +$$

$$+ \int_0^t e^{-\mathbf{k}^2(t-s)} \sum_{p=2}^{\infty} A^p g^{(p)}(\mathbf{k},s)\, ds. \tag{4}$$

The solution of the Burgers equation is written as a series

$$\mathbf{w}^{(A)}(\mathbf{k},t) = A\, e^{-t\mathbf{k}^2}\mathbf{w}^{(1)}(\mathbf{k}) +$$

$$+ \int_0^t e^{-\mathbf{k}^2(t-s)} \sum_{p=2}^{\infty} A^p g^{(p)}(\mathbf{k},s) ds. \tag{4}$$

We find recursive relations in p for $g^{(p)}(\mathbf{k},t)$ which remind of the famous BBGKY hierarchy of statistical physics:

The solution of the Burgers equation is written as a series

$$\mathbf{w}^{(A)}(\mathbf{k},t) = A\, e^{-t\mathbf{k}^2}\mathbf{w}^{(1)}(\mathbf{k}) +$$

$$+\int_0^t e^{-\mathbf{k}^2(t-s)} \sum_{p=2}^{\infty} A^p g^{(p)}(\mathbf{k},s)ds. \tag{4}$$

We find recursive relations in p for $g^{(p)}(\mathbf{k},t)$ which remind of the famous BBGKY hierarchy of statistical physics:
Setting $\mathbf{g}^{(1)}(\mathbf{k},t) = e^{-t\mathbf{k}^2}\mathbf{w}^{(1)}(\mathbf{k})$

The solution of the Burgers equation is written as a series

$$\mathbf{w}^{(A)}(\mathbf{k},t) = A\, e^{-t\mathbf{k}^2}\mathbf{w}^{(1)}(\mathbf{k}) +$$

$$+\int_0^t e^{-\mathbf{k}^2(t-s)}\sum_{p=2}^{\infty} A^p g^{(p)}(\mathbf{k},s)ds. \tag{4}$$

We find recursive relations in p for $g^{(p)}(\mathbf{k},t)$ which remind of the famous BBGKY hierarchy of statistical physics:
Setting $\mathbf{g}^{(1)}(\mathbf{k},t) = e^{-t\mathbf{k}^2}\mathbf{w}^{(1)}(\mathbf{k})$ and

$$\mathbf{g}^{(2)}(\mathbf{k},t) = \int_{\mathbb{R}^2}\langle \mathbf{w}^{(1)}(k-k^{'},s),\mathbf{k}^{'}\rangle \mathbf{w}^{(1)}(\mathbf{k}^{'},s)e^{-t(\mathbf{k}-\mathbf{k}^{'})^2 - t(\mathbf{k}^{'})^2} d\mathbf{k}^{'},$$

we find for $p > 2$ the recursive relations

$$\mathbf{g}^{(p)}(\mathbf{k},t)=\int_0^t ds_2\cdot$$

$$\cdot\int_{\mathbb{R}^2}\langle\mathbf{w}^{(1)}(k-k^{'},s),\mathbf{k}^{'}\rangle\mathbf{g}^{(p-1)}(\mathbf{k}^{'},s)e^{-t(\mathbf{k}-\mathbf{k}^{'})^2-t(\mathbf{k}^{'})^2}d\mathbf{k}^{'},+$$

$$\mathbf{g}^{(p)}(\mathbf{k},t)=\int_0^t ds_2\cdot$$

$$\cdot\int_{\mathbb{R}^2}\langle \mathbf{w}^{(1)}(k-k^{'},s),\mathbf{k}^{'}\rangle \mathbf{g}^{(p-1)}(\mathbf{k}^{'},s)e^{-t(\mathbf{k}-\mathbf{k}^{'})^2-t(\mathbf{k}^{'})^2}d\mathbf{k}^{'},+$$

$$+\sum_{\substack{p_1+p_2=p\\ p_1,p_2>1}}\int_0^t ds_1\int_0^t ds_2\cdot \tag{5}$$

$$\cdot\int_{\mathbb{R}^2}\langle \mathbf{g}^{(p_1)}(\mathbf{k}-\mathbf{k}^{'},s_1),\mathbf{k}^{'}\rangle \mathbf{g}^{(p_2)}(\mathbf{k}^{'},s_2)e^{-(t-s_1)(\mathbf{k}-\mathbf{k}^{'})^2-(t-s_2)(\mathbf{k}^{'})^2}d\mathbf{k}^{'}+$$

$$+\int_0^t ds_1\int_{\mathbb{R}^2}\langle \mathbf{g}^{(p-1)}(\mathbf{k}-\mathbf{k}^{'},s_1),\mathbf{k}^{'}\rangle \mathbf{w}_1(\mathbf{k}^{'})e^{-(t-s_1)(\mathbf{k}-\mathbf{k}^{'})^2-t(\mathbf{k}^{'})^2}d\mathbf{k}^{'}$$

The main contribution to the integrals in ds_1, ds_2 comes from a small neighborhood of the upper bound t.

The main contribution to the integrals in ds_1, ds_2 comes from a small neighborhood of the upper bound t.

This is due to viscosity and would not apply to the Euler system.

The main contribution to the integrals in ds_1, ds_2 comes from a small neighborhood of the upper bound t.

This is due to viscosity and would not apply to the Euler system.

A scaling transformation of $\mathbf{k}$ and the function $\mathbf{g}^{(p)}$ greatly simplifies the asymptotics for large p of the recursive equations.

The main contribution to the integrals in ds_1, ds_2 comes from a small neighborhood of the upper bound t.

This is due to viscosity and would not apply to the Euler system.

A scaling transformation of $\mathbf{k}$ and the function $\mathbf{g}^{(p)}$ greatly simplifies the asymptotics for large p of the recursive equations.

We set $\mathbf{k} = p\mathbf{k}^{(0)} + \sqrt{pa}\,\mathbf{Y}$ and

The main contribution to the integrals in ds_1, ds_2 comes from a small neighborhood of the upper bound t.

This is due to viscosity and would not apply to the Euler system.

A scaling transformation of $\mathbf{k}$ and the function $\mathbf{g}^{(p)}$ greatly simplifies the asymptotics for large p of the recursive equations. We set $\mathbf{k} = p\mathbf{k}^{(0)} + \sqrt{pa}\,\mathbf{Y}$ and

$$\mathbf{h}^{(p)}(Y, t) = \mathbf{g}^{(p)}(p\mathbf{k}^{(0)} + \sqrt{pa}\mathbf{Y}, s), \qquad \mathbf{Y} \in \mathbb{R}^2. \qquad (6).$$

The main contribution to the integrals in ds_1, ds_2 comes from a small neighborhood of the upper bound t.

This is due to viscosity and would not apply to the Euler system.

A scaling transformation of $\mathbf{k}$ and the function $\mathbf{g}^{(p)}$ greatly simplifies the asymptotics for large p of the recursive equations. We set $\mathbf{k} = p\mathbf{k}^{(0)} + \sqrt{pa}\,\mathbf{Y}$ and

$$\mathbf{h}^{(p)}(Y,t) = \mathbf{g}^{(p)}(p\mathbf{k}^{(0)} + \sqrt{pa}\mathbf{Y}, s), \qquad \mathbf{Y} \in \mathbb{R}^2. \qquad (6).$$

For large p the functions $\mathbf{h}^{(p)}$ are concentrated around $|\mathbf{Y}| \approx 1$

The main contribution to the integrals in ds_1, ds_2 comes from a small neighborhood of the upper bound t.

This is due to viscosity and would not apply to the Euler system.

A scaling transformation of $\mathbf{k}$ and the function $\mathbf{g}^{(p)}$ greatly simplifies the asymptotics for large p of the recursive equations. We set $\mathbf{k} = p\mathbf{k}^{(0)} + \sqrt{pa}\,\mathbf{Y}$ and

$$\mathbf{h}^{(p)}(Y,t) = \mathbf{g}^{(p)}(p\mathbf{k}^{(0)} + \sqrt{pa}\mathbf{Y}, s), \qquad \mathbf{Y} \in \mathbb{R}^2. \qquad (6).$$

For large p the functions $\mathbf{h}^{(p)}$ are concentrated around $|\mathbf{Y}| \approx 1$ and we can neglect the first and third term of the recursive relation (5).

The main contribution to the integrals in ds_1, ds_2 comes from a small neighborhood of the upper bound t.

This is due to viscosity and would not apply to the Euler system.

A scaling transformation of $\mathbf{k}$ and the function $\mathbf{g}^{(p)}$ greatly simplifies the asymptotics for large p of the recursive equations. We set $\mathbf{k} = p\mathbf{k}^{(0)} + \sqrt{pa}\,\mathbf{Y}$ and

$$\mathbf{h}^{(p)}(Y, t) = \mathbf{g}^{(p)}(p\mathbf{k}^{(0)} + \sqrt{pa}\mathbf{Y}, s), \qquad \mathbf{Y} \in \mathbb{R}^2. \qquad (6).$$

For large p the functions $\mathbf{h}^{(p)}$ are concentrated around $|\mathbf{Y}| \approx 1$ and we can neglect the first and third term of the recursive relation (5). We also neglect terms like $\frac{\mathbf{Y}'}{\sqrt{p}}$ in the exponent,

The main contribution to the integrals in ds_1, ds_2 comes from a small neighborhood of the upper bound t.

This is due to viscosity and would not apply to the Euler system.

A scaling transformation of $\mathbf{k}$ and the function $\mathbf{g}^{(p)}$ greatly simplifies the asymptotics for large p of the recursive equations. We set $\mathbf{k} = p\mathbf{k}^{(0)} + \sqrt{pa}\,\mathbf{Y}$ and

$$\mathbf{h}^{(p)}(Y, t) = \mathbf{g}^{(p)}(p\mathbf{k}^{(0)} + \sqrt{pa}\mathbf{Y}, s), \qquad \mathbf{Y} \in \mathbb{R}^2. \qquad (6).$$

For large p the functions $\mathbf{h}^{(p)}$ are concentrated around $|\mathbf{Y}| \approx 1$ and we can neglect the first and third term of the recursive relation (5). We also neglect terms like $\frac{\mathbf{Y}'}{\sqrt{p}}$ in the exponent, and introduce the adapted variables

$$s_j = s(1 - \theta_j/p_j^2), \quad j = 1, 2, \qquad \gamma = p_1/p, p_2/p = 1 - \gamma.$$

Setting $\mathbf{k}' = p_2\mathbf{k}^{(0)} + \sqrt{pa}\mathbf{Y}'$, we finally get the simple recursive relation

Setting $\mathbf{k}' = p_2\mathbf{k}^{(0)} + \sqrt{pa}\mathbf{Y}'$, we finally get the simple recursive relation

$$\mathbf{h}^{(p)}(\mathbf{Y},t) = \frac{p^2}{4a^2}\cdot \tag{7}$$

$$\cdot \sum_{\substack{p_1+p_2=p\\ p_1,p_2>1}} \frac{1}{p_1^2 p_2^2} \int_{\mathbb{R}^2} \frac{p_2}{p} \sum_{j=1}^{2} h_j^{(p_1)}\left(\frac{\mathbf{Y}-\mathbf{Y}'}{\sqrt{\gamma}},t\right)\mathbf{h}^{(p_2)}\left(\frac{\mathbf{Y}'}{\sqrt{1-\gamma}},t\right)d\mathbf{Y}'.$$

Setting $\mathbf{k}' = p_2\mathbf{k}^{(0)} + \sqrt{pa}\mathbf{Y}'$, we finally get the simple recursive relation

$$\mathbf{h}^{(p)}(\mathbf{Y}, t) = \frac{p^2}{4a^2} \cdot \tag{7}$$

$$\cdot \sum_{\substack{p_1+p_2=p \\ p_1,p_2>1}} \frac{1}{p_1^2 p_2^2} \int_{\mathbb{R}^2} \frac{p_2}{p} \sum_{j=1}^{2} h_j^{(p_1)}\left(\frac{\mathbf{Y}-\mathbf{Y}'}{\sqrt{\gamma}}, t\right) \mathbf{h}^{(p_2)}\left(\frac{\mathbf{Y}'}{\sqrt{1-\gamma}}, t\right) d\mathbf{Y}'.$$

By induction, assume that there are nested time intervals $\mathcal{J}^{(p+1)} \subseteq \mathcal{J}^{(p)}$, such that for $t \in \mathcal{J}^{(p)}$,

$$\mathbf{h}^{(r)}(\mathbf{Y}, t) = r\, Z(t)(\Lambda_p(t))^r \frac{e^{-\frac{\mathbf{Y}^2}{2\sigma^2}}}{2\pi\sigma^2} \left(\mathbf{H}(\mathbf{Y}) + \delta_r(\mathbf{Y}, t)\right), \tag{8}$$

for some some $\sigma > 0$ and all $r < p$,

Setting $\mathbf{k}' = p_2\mathbf{k}^{(0)} + \sqrt{pa}\mathbf{Y}'$, we finally get the simple recursive relation

$$\mathbf{h}^{(p)}(\mathbf{Y},t) = \frac{p^2}{4a^2}\cdot \tag{7}$$

$$\cdot \sum_{\substack{p_1+p_2=p\\ p_1,p_2>1}} \frac{1}{p_1^2 p_2^2} \int_{\mathbb{R}^2} \frac{p_2}{p} \sum_{j=1}^{2} h_j^{(p_1)}\left(\frac{\mathbf{Y}-\mathbf{Y}'}{\sqrt{\gamma}},t\right) \mathbf{h}^{(p_2)}\left(\frac{\mathbf{Y}'}{\sqrt{1-\gamma}},t\right) d\mathbf{Y}'.$$

By induction, assume that there are nested time intervals $\mathcal{J}^{(p+1)} \subseteq \mathcal{J}^{(p)}$, such that for $t \in \mathcal{J}^{(p)}$,

$$\mathbf{h}^{(r)}(\mathbf{Y},t) = r\, Z(t)(\Lambda_p(t))^r \frac{e^{-\frac{\mathbf{Y}^2}{2\sigma^2}}}{2\pi\sigma^2} \left(\mathbf{H}(\mathbf{Y}) + \delta_r(\mathbf{Y},t)\right), \tag{8}$$

for some some $\sigma > 0$ and all $r < p$, where δ_r is small and Z, Λ_p are functions to be determined.

As $p \to \infty$ the sum in (7) is a Riemann sum with step $\frac{1}{p}$.

As $p \to \infty$ the sum in (7) is a Riemann sum with step $\frac{1}{p}$. Assuming that near the critical time $Z(t) = 4a^2$, we get for $\mathbf{H}$ the equation

As $p \to \infty$ the sum in (7) is a Riemann sum with step $\frac{1}{p}$. Assuming that near the critical time $Z(t) = 4a^2$, we get for $\mathbf{H}$ the equation

$$\mathbf{H}(\mathbf{Y}) \frac{e^{-\frac{\mathbf{Y}^2}{2\sigma^2}}}{2\pi\sigma^2} = \int_0^1 d\gamma (1-\gamma) \int_{\mathbb{R}^2} d\mathbf{Y}' \mathbf{H}\left(\frac{\mathbf{Y}'}{\sqrt{1-\gamma}}\right) \cdot \tag{9}$$

$$\cdot \left[H_1\left(\frac{\mathbf{Y}-\mathbf{Y}'}{\sqrt{\gamma}}\right) + H_2\left(\frac{\mathbf{Y}-\mathbf{Y}'}{\sqrt{\gamma}}\right)\right] \frac{e^{-\frac{(\mathbf{Y}-\mathbf{Y}')^2}{2\sigma^2\gamma}}}{2\pi\sigma^2\gamma} \frac{e^{-\frac{(\mathbf{Y}')^2}{2\sigma^2(1-\gamma)}}}{2\pi\sigma^2(1-\gamma)}.$$

As $p \to \infty$ the sum in (7) is a Riemann sum with step $\frac{1}{p}$. Assuming that near the critical time $Z(t) = 4a^2$, we get for $\mathbf{H}$ the equation

$$\mathbf{H}(\mathbf{Y}) \frac{e^{-\frac{\mathbf{Y}^2}{2\sigma^2}}}{2\pi\sigma^2} = \int_0^1 d\gamma (1-\gamma) \int_{\mathbb{R}^2} d\mathbf{Y}' \mathbf{H}\left(\frac{\mathbf{Y}'}{\sqrt{1-\gamma}}\right) \cdot \tag{9}$$

$$\cdot \left[H_1\left(\frac{\mathbf{Y}-\mathbf{Y}'}{\sqrt{\gamma}}\right) + H_2\left(\frac{\mathbf{Y}-\mathbf{Y}'}{\sqrt{\gamma}}\right)\right] \frac{e^{-\frac{(\mathbf{Y}-\mathbf{Y}')^2}{2\sigma^2\gamma}}}{2\pi\sigma^2\gamma} \frac{e^{-\frac{(\mathbf{Y}')^2}{2\sigma^2(1-\gamma)}}}{2\pi\sigma^2(1-\gamma)}.$$

It is a fixed point equation, which, as usual in the renormalization group method, is of fundamental importance.

As $p \to \infty$ the sum in (7) is a Riemann sum with step $\frac{1}{p}$.
Assuming that near the critical time $Z(t) = 4a^2$, we get for $\mathbf{H}$ the equation

$$\mathbf{H}(\mathbf{Y})\frac{e^{-\frac{\mathbf{Y}^2}{2\sigma^2}}}{2\pi\sigma^2} = \int_0^1 d\gamma(1-\gamma)\int_{\mathbb{R}^2} d\mathbf{Y}'\mathbf{H}\left(\frac{\mathbf{Y}'}{\sqrt{1-\gamma}}\right)\cdot \qquad (9)$$

$$\cdot\left[H_1\left(\frac{\mathbf{Y}-\mathbf{Y}'}{\sqrt{\gamma}}\right) + H_2\left(\frac{\mathbf{Y}-\mathbf{Y}'}{\sqrt{\gamma}}\right)\right]\frac{e^{-\frac{(\mathbf{Y}-\mathbf{Y}')^2}{2\sigma^2\gamma}}}{2\pi\sigma^2\gamma}\frac{e^{-\frac{(\mathbf{Y}')^2}{2\sigma^2(1-\gamma)}}}{2\pi\sigma^2(1-\gamma)}.$$

It is a fixed point equation, which, as usual in the renormalization group method, is of fundamental importance.

(For the NS equations the corresponding equation is more complicated.)

As $p \to \infty$ the sum in (7) is a Riemann sum with step $\frac{1}{p}$. Assuming that near the critical time $Z(t) = 4a^2$, we get for $\mathbf{H}$ the equation

$$\mathbf{H}(\mathbf{Y})\frac{e^{-\frac{\mathbf{Y}^2}{2\sigma^2}}}{2\pi\sigma^2} = \int_0^1 d\gamma(1-\gamma)\int_{\mathbb{R}^2} d\mathbf{Y}^{'}\mathbf{H}\left(\frac{\mathbf{Y}^{'}}{\sqrt{1-\gamma}}\right)\cdot \tag{9}$$

$$\cdot \left[H_1\left(\frac{\mathbf{Y}-\mathbf{Y}^{'}}{\sqrt{\gamma}}\right) + H_2\left(\frac{\mathbf{Y}-\mathbf{Y}^{'}}{\sqrt{\gamma}}\right)\right]\frac{e^{-\frac{(\mathbf{Y}-\mathbf{Y}^{'})^2}{2\sigma^2\gamma}}}{2\pi\sigma^2\gamma}\frac{e^{-\frac{(\mathbf{Y}^{'})^2}{2\sigma^2(1-\gamma)}}}{2\pi\sigma^2(1-\gamma)}.$$

It is a fixed point equation, which, as usual in the renormalization group method, is of fundamental importance. (For the NS equations the corresponding equation is more complicated.)

Equation (9) admits the constant solution $\mathbf{H}_0(\mathbf{Y}) = (1,1)$.

By linearizing around $\mathbf{H}_0(\mathbf{Y})$ and expanding in the Hermite polynomials one can see that there is a 2-dimensional unstable subspace and a 4-dimensional neutral one.

By linearizing around $\mathbf{H}_0(\mathbf{Y})$ and expanding in the Hermite polynomials one can see that there is a 2-dimensional unstable subspace and a 4-dimensional neutral one.

All directions orthogonal to such subspaces in the L_2 space $\mathcal{H}$ with norm (3) are stable.

By linearizing around $\mathbf{H}_0(\mathbf{Y})$ and expanding in the Hermite polynomials one can see that there is a 2-dimensional unstable subspace and a 4-dimensional neutral one.

All directions orthogonal to such subspaces in the L_2 space $\mathcal{H}$ with norm (3) are stable.

The parameters B and $\mathbf{b}$ in the initial data determine the projection on the unstable and neutral subspaces.

By linearizing around $\mathbf{H}_0(\mathbf{Y})$ and expanding in the Hermite polynomials one can see that there is a 2-dimensional unstable subspace and a 4-dimensional neutral one.

All directions orthogonal to such subspaces in the L_2 space $\mathcal{H}$ with norm (3) are stable.

The parameters B and $\mathbf{b}$ in the initial data determine the projection on the unstable and neutral subspaces.

The term with the vector function (ϕ_1, ϕ_2) is the stable component.

By linearizing around $\mathbf{H}_0(\mathbf{Y})$ and expanding in the Hermite polynomials one can see that there is a 2-dimensional unstable subspace and a 4-dimensional neutral one.

All directions orthogonal to such subspaces in the L_2 space $\mathcal{H}$ with norm (3) are stable.

The parameters B and $\mathbf{b}$ in the initial data determine the projection on the unstable and neutral subspaces.

The term with the vector function (ϕ_1, ϕ_2) is the stable component.

Setting $\mathbf{H} = \mathbf{H}_0$ in equation (8), we have to find intervals $\mathcal{J}^{(p)}$ with a nonempty interval $\mathcal{J}$ as intersection, such that for $t \in \mathcal{J}$ the remainder δ_r tends to zero for large r.

By linearizing around $\mathbf{H}_0(\mathbf{Y})$ and expanding in the Hermite polynomials one can see that there is a 2-dimensional unstable subspace and a 4-dimensional neutral one.

All directions orthogonal to such subspaces in the L_2 space $\mathcal{H}$ with norm (3) are stable.

The parameters B and $\mathbf{b}$ in the initial data determine the projection on the unstable and neutral subspaces.

The term with the vector function (ϕ_1, ϕ_2) is the stable component.

Setting $\mathbf{H} = \mathbf{H}_0$ in equation (8), we have to find intervals $\mathcal{J}^{(p)}$ with a nonempty interval $\mathcal{J}$ as intersection, such that for $t \in \mathcal{J}$ the remainder δ_r tends to zero for large r.

We need to control the components of δ_r along the unstable and neutral subspaces when we iterate in r. (The stable component vanishes exponentially fast.)

A delicate analysis shows that for large p we have $\Lambda_p(t) \approx \Lambda(t)$, with Λ a monotonic positive function.

A delicate analysis shows that for large p we have $\Lambda_p(t) \approx \Lambda(t)$, with Λ a monotonic positive function.

Therefore by choosing $A = \frac{1}{\Lambda(\tau)}$ one gets a solution blowing up at some time $\tau \in \mathcal{J}$.

A delicate analysis shows that for large p we have $\Lambda_p(t) \approx \Lambda(t)$, with Λ a monotonic positive function.

Therefore by choosing $A = \frac{1}{\Lambda(\tau)}$ one gets a solution blowing up at some time $\tau \in \mathcal{J}$.

In fact, the main contribution to the integral in (4) comes for $s \approx t$.

A delicate analysis shows that for large p we have $\Lambda_p(t) \approx \Lambda(t)$, with Λ a monotonic positive function.

Therefore by choosing $A = \frac{1}{\Lambda(\tau)}$ one gets a solution blowing up at some time $\tau \in \mathcal{J}$.

In fact, the main contribution to the integral in (4) comes for $s \approx t$. Hence, by (8), the solution near the critical time τ is approximately given by

A delicate analysis shows that for large p we have $\Lambda_p(t) \approx \Lambda(t)$, with Λ a monotonic positive function.

Therefore by choosing $A = \frac{1}{\Lambda(\tau)}$ one gets a solution blowing up at some time $\tau \in \mathcal{J}$.

In fact, the main contribution to the integral in (4) comes for $s \approx t$. Hence, by (8), the solution near the critical time τ is approximately given by

$$\sum_p A^p \mathbf{g}^{(p)}(\mathbf{k}, t) \approx C \sum_p p \left(\frac{\Lambda(t)}{\Lambda(\tau)} \right)^p \frac{e^{-\frac{(\mathbf{k} - p\mathbf{k}^{(0)})^2}{2ap\sigma^2}}}{2\pi\sigma^2} \mathbf{H}_0(\mathbf{Y}), \qquad (10).$$

where C is a constant.

So we have divergence when $t \uparrow \tau$ near the point $\mathbf{k} = p\,\mathbf{k}^{(0)}$.

A delicate analysis shows that for large p we have $\Lambda_p(t) \approx \Lambda(t)$, with Λ a monotonic positive function.

Therefore by choosing $A = \frac{1}{\Lambda(\tau)}$ one gets a solution blowing up at some time $\tau \in \mathcal{J}$.

In fact, the main contribution to the integral in (4) comes for $s \approx t$. Hence, by (8), the solution near the critical time τ is approximately given by

$$\sum_p A^p \mathbf{g}^{(p)}(\mathbf{k}, t) \approx C \sum_p p \left(\frac{\Lambda(t)}{\Lambda(\tau)} \right)^p \frac{e^{-\frac{(\mathbf{k} - p\mathbf{k}^{(0)})^2}{2ap\sigma^2}}}{2\pi\sigma^2} \mathbf{H}_0(\mathbf{Y}), \qquad (10).$$

where C is a constant.

So we have divergence when $t \uparrow \tau$ near the point $\mathbf{k} = p\,\mathbf{k}^{(0)}$.

The approximate expression (10) allows us to predict the main features of the solution.

A delicate analysis shows that for large p we have $\Lambda_p(t) \approx \Lambda(t)$, with Λ a monotonic positive function.

Therefore by choosing $A = \frac{1}{\Lambda(\tau)}$ one gets a solution blowing up at some time $\tau \in \mathcal{J}$.

In fact, the main contribution to the integral in (4) comes for $s \approx t$. Hence, by (8), the solution near the critical time τ is approximately given by

$$\sum_p A^p \mathbf{g}^{(p)}(\mathbf{k}, t) \approx C \sum_p p \left(\frac{\Lambda(t)}{\Lambda(\tau)} \right)^p \frac{e^{-\frac{(\mathbf{k} - p\mathbf{k}^{(0)})^2}{2ap\sigma^2}}}{2\pi\sigma^2} \mathbf{H}_0(\mathbf{Y}), \qquad (10).$$

where C is a constant.

So we have divergence when $t \uparrow \tau$ near the point $\mathbf{k} = p\,\mathbf{k}^{(0)}$.

The approximate expression (10) allows us to predict the main features of the solution.

For small $\tau - t$ we have $\frac{\Lambda(t)}{\Lambda(\tau)} \approx 1 - \beta(\tau - t)$ for some $\beta > 0$.

For small $\tau - t$ we have $\frac{\Lambda(t)}{\Lambda(\tau)} \approx 1 - \beta(\tau - t)$ for some $\beta > 0$.

Hence the main contribution to the series (10) comes from $p = p(t) \approx \frac{c}{\tau - t}$:

For small $\tau - t$ we have $\frac{\Lambda(t)}{\Lambda(\tau)} \approx 1 - \beta(\tau - t)$ for some $\beta > 0$.

Hence the main contribution to the series (10) comes from $p = p(t) \approx \frac{c}{\tau - t}$: the support of the solution in k-space escapes to infinity along the direction $(1,1)$ as $t \uparrow \tau$.

For small $\tau - t$ we have $\frac{\Lambda(t)}{\Lambda(\tau)} \approx 1 - \beta(\tau - t)$ for some $\beta > 0$.

Hence the main contribution to the series (10) comes from $p = p(t) \approx \frac{c}{\tau - t}$: the support of the solution in k-space escapes to infinity along the direction $(1,1)$ as $t \uparrow \tau$.

A simple analysis shows that the total energy

$$E(t) = \int_{\mathbb{R}^2} |\mathbf{v}(\mathbf{k},t)|^2 d\mathbf{k}$$

For small $\tau - t$ we have $\frac{\Lambda(t)}{\Lambda(\tau)} \approx 1 - \beta(\tau - t)$ for some $\beta > 0$.

Hence the main contribution to the series (10) comes from $p = p(t) \approx \frac{c}{\tau - t}$: the support of the solution in k-space escapes to infinity along the direction $(1,1)$ as $t \uparrow \tau$.

A simple analysis shows that the total energy

$$E(t) = \int_{\mathbb{R}^2} |\mathbf{v}(\mathbf{k},t)|^2 d\mathbf{k}$$

behaves near the critical time τ as

$$E(t) \sim \frac{C_E}{(\tau - t)^5}, \qquad C_E > 0. \tag{11}$$

For small $\tau - t$ we have $\frac{\Lambda(t)}{\Lambda(\tau)} \approx 1 - \beta(\tau - t)$ for some $\beta > 0$.

Hence the main contribution to the series (10) comes from $p = p(t) \approx \frac{c}{\tau - t}$: the support of the solution in k-space escapes to infinity along the direction $(1, 1)$ as $t \uparrow \tau$.

A simple analysis shows that the total energy

$$E(t) = \int_{\mathbb{R}^2} |\mathbf{v}(\mathbf{k}, t)|^2 d\mathbf{k}$$

behaves near the critical time τ as

$$E(t) \sim \frac{C_E}{(\tau - t)^5}, \qquad C_E > 0. \tag{11}$$

The inverse Fourier transform, i.e., the solution in $\mathbf{x}$-space

$$\mathbf{u}(\mathbf{x}, t) = -\frac{i}{2\pi} \int_{\mathbb{R}^2} \mathbf{v}(\mathbf{k}, t) e^{-i\langle \mathbf{k}, \mathbf{x} \rangle} d\mathbf{k}$$

converges as $t \uparrow \tau$ for all $\mathbf{x} \neq 0$, and diverges at $\mathbf{x} = 0$.

3. RESULTS OF COMPUTER SIMULATIONS

3. RESULTS OF COMPUTER SIMULATIONS

In computer simulations we had to face some characteristic difficulties.

3. RESULTS OF COMPUTER SIMULATIONS

In computer simulations we had to face some characteristic difficulties.

- Instability of the flow at large Reynolds numbers.

3. RESULTS OF COMPUTER SIMULATIONS

In computer simulations we had to face some characteristic difficulties.

- Instability of the flow at large Reynolds numbers.

- The blow-up is very fast: for 2-d Burgers it takes place in a time of the order of $10^{-4} - 10^{-5}$ time units.

3. RESULTS OF COMPUTER SIMULATIONS

In computer simulations we had to face some characteristic difficulties.

- Instability of the flow at large Reynolds numbers.

- The blow-up is very fast: for 2-d Burgers it takes place in a time of the order of $10^{-4} - 10^{-5}$ time units.

- In Fourier space (where we work) the solution moves out to infinity as we approach the critical time τ.

3. RESULTS OF COMPUTER SIMULATIONS

In computer simulations we had to face some characteristic difficulties.

- Instability of the flow at large Reynolds numbers.

- The blow-up is very fast: for 2-d Burgers it takes place in a time of the order of $10^{-4} - 10^{-5}$ time units.

- In Fourier space (where we work) the solution moves out to infinity as we approach the critical time τ.

In the blow-up region the qualitative behavior of the total energy, enstrophy, and other global characteristics is remarkably stable, and does not depend on the mesh size in a rather wide range.

3. RESULTS OF COMPUTER SIMULATIONS

In computer simulations we had to face some characteristic difficulties.

- Instability of the flow at large Reynolds numbers.

- The blow-up is very fast: for 2-d Burgers it takes place in a time of the order of $10^{-4} - 10^{-5}$ time units.

- In Fourier space (where we work) the solution moves out to infinity as we approach the critical time τ.

In the blow-up region the qualitative behavior of the total energy, enstrophy, and other global characteristics is remarkably stable, and does not depend on the mesh size in a rather wide range. The precision, i.e., the control on the actual values of the solutions becomes, as expected, worse, as we approach the explosion time, due to large derivatives.

3. RESULTS OF COMPUTER SIMULATIONS

In computer simulations we had to face some characteristic difficulties.

- Instability of the flow at large Reynolds numbers.

- The blow-up is very fast: for 2-d Burgers it takes place in a time of the order of $10^{-4} - 10^{-5}$ time units.

- In Fourier space (where we work) the solution moves out to infinity as we approach the critical time τ.

In the blow-up region the qualitative behavior of the total energy, enstrophy, and other global characteristics is remarkably stable, and does not depend on the mesh size in a rather wide range. The precision, i.e., the control on the actual values of the solutions becomes, as expected, worse, as we approach the explosion time, due to large derivatives.

Nevertheless, in the first part of the explosion range we have enough precision to allow a reasonable prediction on the value of the explosion time.

The simulations was performed at the CINECA/SCS (SuperComputingSolution) Center at Bologna on the Supercomputer IBM SP6.

The simulations was performed at the CINECA/SCS (SuperComputingSolution) Center at Bologna on the Supercomputer IBM SP6.

The computations were implemented by a trapezoidal Crank-Nicholson Algorithm, both explicit and implicit.

The simulations was performed at the CINECA/SCS (SuperComputingSolution) Center at Bologna on the Supercomputer IBM SP6.

The computations were implemented by a trapezoidal Crank-Nicholson Algorithm, both explicit and implicit.

Convolutions are computed by a discrete fast Fourier transform algorithm.

The simulations was performed at the CINECA/SCS (SuperComputingSolution) Center at Bologna on the Supercomputer IBM SP6.

The computations were implemented by a trapezoidal Crank-Nicholson Algorithm, both explicit and implicit.

Convolutions are computed by a discrete fast Fourier transform algorithm.

The mesh of the space points was adapted in order to cover the region with significant values of the solutions.

The simulations was performed at the CINECA/SCS (SuperComputingSolution) Center at Bologna on the Supercomputer IBM SP6.

The computations were implemented by a trapezoidal Crank-Nicholson Algorithm, both explicit and implicit.

Convolutions are computed by a discrete fast Fourier transform algorithm.

The mesh of the space points was adapted in order to cover the region with significant values of the solutions.

The results of our computer simulations are in full accordance with the theoretical predictions.

The simulations was performed at the CINECA/SCS (SuperComputingSolution) Center at Bologna on the Supercomputer IBM SP6.

The computations were implemented by a trapezoidal Crank-Nicholson Algorithm, both explicit and implicit.

Convolutions are computed by a discrete fast Fourier transform algorithm.

The mesh of the space points was adapted in order to cover the region with significant values of the solutions.

The results of our computer simulations are in full accordance with the theoretical predictions.

They also give additional information on the behavior of the solutions near the singular time τ.

The simulations was performed at the CINECA/SCS (SuperComputingSolution) Center at Bologna on the Supercomputer IBM SP6.

The computations were implemented by a trapezoidal Crank-Nicholson Algorithm, both explicit and implicit.

Convolutions are computed by a discrete fast Fourier transform algorithm.

The mesh of the space points was adapted in order to cover the region with significant values of the solutions.

The results of our computer simulations are in full accordance with the theoretical predictions.

They also give additional information on the behavior of the solutions near the singular time τ.

For the initial condition (2a,b), we took $\sigma^2 = 5$, $\mathbf{k}^0 = (5, 5)$, or $a = 5$, and

$$\phi^{(1)}(\mathbf{k}) = \phi^{(2)}(\mathbf{k}) = a_1(k_1^2 - 5) + a_2(k_2^2 - 5) + a_3 k_1 k_2.$$

We first did a rough screening of the solutions generated by 50,000 initial data, obtained by a random choice of the parameters:

We first did a rough screening of the solutions generated by 50,000 initial data, obtained by a random choice of the parameters: for the constant B in the interval $(5, 50)$, and for the five components of $\mathbf{b}$ and the constants a_1, a_2, a_3 in a small interval around the origin.

We first did a rough screening of the solutions generated by 50,000 initial data, obtained by a random choice of the parameters: for the constant B in the interval $(5, 50)$, and for the five components of $\mathbf{b}$ and the constants a_1, a_2, a_3 in a small interval around the origin.

The solutions were followed up on a space-time mesh with space step $\delta_k = 0.5$ and time step $\delta_t = 10^{-4}$ for 100 time steps.

We first did a rough screening of the solutions generated by 50,000 initial data, obtained by a random choice of the parameters: for the constant B in the interval $(5, 50)$, and for the five components of $\mathbf{b}$ and the constants a_1, a_2, a_3 in a small interval around the origin.

The solutions were followed up on a space-time mesh with space step $\delta_k = 0.5$ and time step $\delta_t = 10^{-4}$ for 100 time steps.

16 cases, with evidence of growing energy, were followed up with a smaller time steps. Most of them did in fact show a blow-up, with a very short explosion time $\Delta \approx 5 \cdot 10^{-5}$.

We report the results for one particular case, corresponding to the following choice of the parameters: $B = 49.36$ and

$$b_0 = 0.02, \quad b_1^{(1)} = 0.09, b_2^{(1)} = 0.02, \quad b_1^{(2)} = -0.12, b_2^{(2)} = 0.09$$

$$a_1 = 0.11, \quad a_2 = 0.12, \quad a_3 = 0.11.$$

The solution explodes at a time $\tau \approx 12 \cdot 10^{-4}$.

The solution explodes at a time $\tau \approx 12 \cdot 10^{-4}$. The energy at first decreases slowly, and then it explodes in a time of order Δ.

The solution explodes at a time $\tau \approx 12 \cdot 10^{-4}$. The energy at first decreases slowly, and then it explodes in a time of order Δ.

For convenience, we rotated the initial data so that the solution moves out to infinity along the k_1 axis.

The solution explodes at a time $\tau \approx 12 \cdot 10^{-4}$. The energy at first decreases slowly, and then it explodes in a time of order Δ.

For convenience, we rotated the initial data so that the solution moves out to infinity along the k_1 axis.

The solution was followed up only as long as the range of the significant data was within the computation region.

The solution explodes at a time $\tau \approx 12 \cdot 10^{-4}$. The energy at first decreases slowly, and then it explodes in a time of order Δ.

For convenience, we rotated the initial data so that the solution moves out to infinity along the k_1 axis.

The solution was followed up only as long as the range of the significant data was within the computation region.

For a detailed study we used three values of the time step

$$\delta_t = 2^{-7} \cdot 10^{-4}, \quad \delta_t = 2^{-8} \cdot 10^{-4}, \quad \delta_t = 2^{-9} \cdot 10^{-4},$$

and three values of the space step

$$\delta_k = 0.5, \quad \delta_k = 1, \quad \delta_k = 2.$$

The solution explodes at a time $\tau \approx 12 \cdot 10^{-4}$. The energy at first decreases slowly, and then it explodes in a time of order Δ.

For convenience, we rotated the initial data so that the solution moves out to infinity along the k_1 axis.

The solution was followed up only as long as the range of the significant data was within the computation region.

For a detailed study we used three values of the time step

$$\delta_t = 2^{-7} \cdot 10^{-4}, \quad \delta_t = 2^{-8} \cdot 10^{-4}, \quad \delta_t = 2^{-9} \cdot 10^{-4},$$

and three values of the space step

$$\delta_k = 0.5, \quad \delta_k = 1, \quad \delta_k = 2.$$

As predicted by the theory, near the blow-up time τ the energy behaves as $(\tau - t)^{-5}$,

The solution explodes at a time $\tau \approx 12 \cdot 10^{-4}$. The energy at first decreases slowly, and then it explodes in a time of order Δ.

For convenience, we rotated the initial data so that the solution moves out to infinity along the k_1 axis.

The solution was followed up only as long as the range of the significant data was within the computation region.

For a detailed study we used three values of the time step

$$\delta_t = 2^{-7} \cdot 10^{-4}, \quad \delta_t = 2^{-8} \cdot 10^{-4}, \quad \delta_t = 2^{-9} \cdot 10^{-4},$$

and three values of the space step

$$\delta_k = 0.5, \quad \delta_k = 1, \quad \delta_k = 2.$$

As predicted by the theory, near the blow-up time τ the energy behaves as $(\tau - t)^{-5}$, so that τ can be identified as the intercept of the function $(E(t))^{-\frac{1}{5}}$ with the time axis.

Evaluation of the explosion time τ:

Evaluation of the explosion time τ:

δ_t	$2^{-7} \cdot 10^{-4}$	$2^{-8} \cdot 10^{-4}$	$2^{-9} \cdot 10^{-4}$
Exp $\delta_{\mathbf{k}} = .5$	$12.666 \cdot 10^{-4}$	$12.387 \cdot 10^{-4}$	
Exp $\delta_{\mathbf{k}} = 1$	$12.668 \cdot 10^{-4}$	$12.400 \cdot 10^{-4}$	$12.215 \cdot 10^{-4}$
Imp $\delta_{\mathbf{k}} = 1$	$12.132 \cdot 10^{-4}$	$12.028 \cdot 10^{-4}$	
Imp $\delta_{\mathbf{k}} = 2$	$12.104 \cdot 10^{-4}$	$12.016 \cdot 10^{-4}$	

Table: *Value of the "explosion" time τ for the different choices of δ_t, of δ_k and the explicit (Exp) or implicit (Imp) integration method.*

Evaluation of the explosion time τ:

δ_t	$2^{-7} \cdot 10^{-4}$	$2^{-8} \cdot 10^{-4}$	$2^{-9} \cdot 10^{-4}$
Exp $\delta_\mathbf{k} = .5$	$12.666 \cdot 10^{-4}$	$12.387 \cdot 10^{-4}$	
Exp $\delta_\mathbf{k} = 1$	$12.668 \cdot 10^{-4}$	$12.400 \cdot 10^{-4}$	$12.215 \cdot 10^{-4}$
Imp $\delta_\mathbf{k} = 1$	$12.132 \cdot 10^{-4}$	$12.028 \cdot 10^{-4}$	
Imp $\delta_\mathbf{k} = 2$	$12.104 \cdot 10^{-4}$	$12.016 \cdot 10^{-4}$	

Table: *Value of the "explosion" time τ for the different choices of δ_t, of δ_k and the explicit (Exp) or implicit (Imp) integration method.*

τ is remarkably stable:

Evaluation of the explosion time τ:

δ_t	$2^{-7} \cdot 10^{-4}$	$2^{-8} \cdot 10^{-4}$	$2^{-9} \cdot 10^{-4}$
Exp $\delta_{\mathbf{k}} = .5$	$12.666 \cdot 10^{-4}$	$12.387 \cdot 10^{-4}$	
Exp $\delta_{\mathbf{k}} = 1$	$12.668 \cdot 10^{-4}$	$12.400 \cdot 10^{-4}$	$12.215 \cdot 10^{-4}$
Imp $\delta_{\mathbf{k}} = 1$	$12.132 \cdot 10^{-4}$	$12.028 \cdot 10^{-4}$	
Imp $\delta_{\mathbf{k}} = 2$	$12.104 \cdot 10^{-4}$	$12.016 \cdot 10^{-4}$	

Table: *Value of the "explosion" time τ for the different choices of δ_t, of δ_k and the explicit (Exp) or implicit (Imp) integration method.*

τ is remarkably stable: it decreases as we refine the mesh, and tends to a limit around $12.0 \cdot 10^{-4}$ time units.

Evaluation of the explosion time τ:

δ_t	$2^{-7} \cdot 10^{-4}$	$2^{-8} \cdot 10^{-4}$	$2^{-9} \cdot 10^{-4}$
Exp $\delta_{\mathbf{k}} = .5$	$12.666 \cdot 10^{-4}$	$12.387 \cdot 10^{-4}$	
Exp $\delta_{\mathbf{k}} = 1$	$12.668 \cdot 10^{-4}$	$12.400 \cdot 10^{-4}$	$12.215 \cdot 10^{-4}$
Imp $\delta_{\mathbf{k}} = 1$	$12.132 \cdot 10^{-4}$	$12.028 \cdot 10^{-4}$	
Imp $\delta_{\mathbf{k}} = 2$	$12.104 \cdot 10^{-4}$	$12.016 \cdot 10^{-4}$	

Table: *Value of the "explosion" time τ for the different choices of δ_t, of δ_k and the explicit (Exp) or implicit (Imp) integration method.*

τ is remarkably stable: it decreases as we refine the mesh, and tends to a limit around $12.0 \cdot 10^{-4}$ time units.

As δ_t decreases, the total energy (at fixed time) increases, and τ decreases, indicating that there are large time derivatives.

Evaluation of the explosion time τ:

δ_t	$2^{-7} \cdot 10^{-4}$	$2^{-8} \cdot 10^{-4}$	$2^{-9} \cdot 10^{-4}$
Exp $\delta_\mathbf{k} = .5$	$12.666 \cdot 10^{-4}$	$12.387 \cdot 10^{-4}$	
Exp $\delta_\mathbf{k} = 1$	$12.668 \cdot 10^{-4}$	$12.400 \cdot 10^{-4}$	$12.215 \cdot 10^{-4}$
Imp $\delta_\mathbf{k} = 1$	$12.132 \cdot 10^{-4}$	$12.028 \cdot 10^{-4}$	
Imp $\delta_\mathbf{k} = 2$	$12.104 \cdot 10^{-4}$	$12.016 \cdot 10^{-4}$	

Table: *Value of the "explosion" time τ for the different choices of δ_t, of δ_k and the explicit (Exp) or implicit (Imp) integration method.*

τ is remarkably stable: it decreases as we refine the mesh, and tends to a limit around $12.0 \cdot 10^{-4}$ time units.

As δ_t decreases, the total energy (at fixed time) increases, and τ decreases, indicating that there are large time derivatives.

Behavior of the total energy for different computational choices: (R-square is always above 0.9973, up to 0.9993).

Behavior of the total energy for different computational choices: (R-square is always above 0.9973, up to 0.9993).

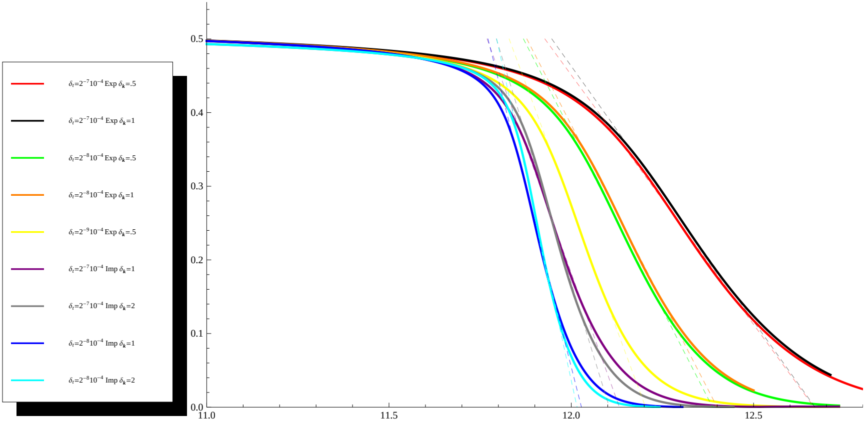

Figure: $(E(t))^{-1/5}$ *versus* $t \cdot 10^4$ *for the different choices of* δ_t, *of* δ_k *and the explicit (Exp) or implicit (Imp) integration method.*

In the energy plot in $\mathbf{k}$-space the blow-up appears as a fast growing bump, moving away along the k_1 axis.

In the energy plot in $\mathbf{k}$-space the blow-up appears as a fast growing bump, moving away along the k_1 axis.

As predicted by the theory, the bump has a peak (global maximum) around some point $\mathbf{K}_M(t) \approx p(t)\mathbf{k}^{(0)}$, for $p(t) \approx \frac{const}{\tau - t}$.

In the energy plot in $\mathbf{k}$-space the blow-up appears as a fast growing bump, moving away along the k_1 axis.

As predicted by the theory, the bump has a peak (global maximum) around some point $\mathbf{K}_M(t) \approx p(t)\mathbf{k}^{(0)}$, for $p(t) \approx \frac{const}{\tau - t}$.

Time	$(\tau - t) \cdot \vert\mathbf{K}_M(t)\vert$
11.9453	425.648
11.9688	406.982
12.0000	362.868
12.0313	300.739
12.0625	223.095

Table: $\delta_t = 2^{-7} \cdot 10^{-4}$, $\delta_{\mathbf{k}} = 1$, implicit integration method. $(\tau - t) \cdot |\mathbf{K}_M(t)|$ versus t, $\tau = 12.132$.

The bump is stretched along the direction of motion, with length of order $1/(\tau - t)$, and transversal dimension is of the order $\frac{1}{\sqrt{\tau - t}}$.

The bump is stretched along the direction of motion, with length of order $1/(\tau - t)$, and transversal dimension is of the order $\frac{1}{\sqrt{\tau - t}}$.

The following slides show how the explosion begins in $\mathbf{k}$-space and in $\mathbf{x}$-space.

The bump is stretched along the direction of motion, with length of order $1/(\tau - t)$, and transversal dimension is of the order $\frac{1}{\sqrt{\tau - t}}$.

The following slides show how the explosion begins in $\mathbf{k}$-space and in $\mathbf{x}$-space.

The scale on the vertical axis is fixed in both cases. For the $\mathbf{x}$-space we plot not the energy $e(\mathbf{k})$, but its logarithm.

T=11,980

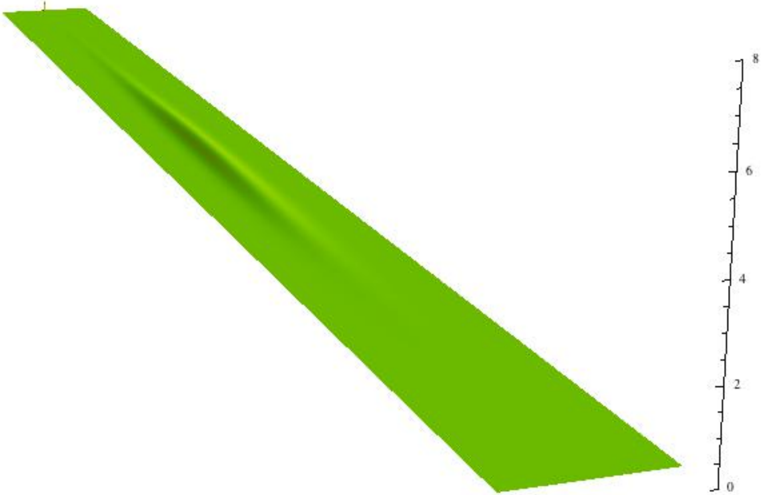

T=12,000

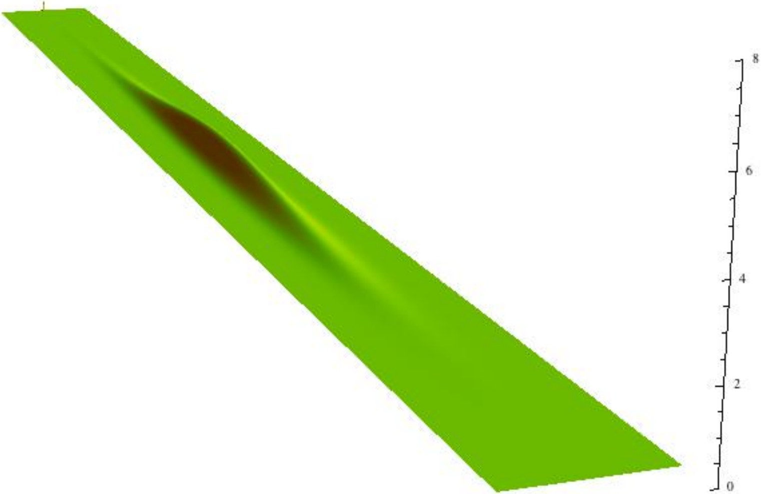

T=12,004

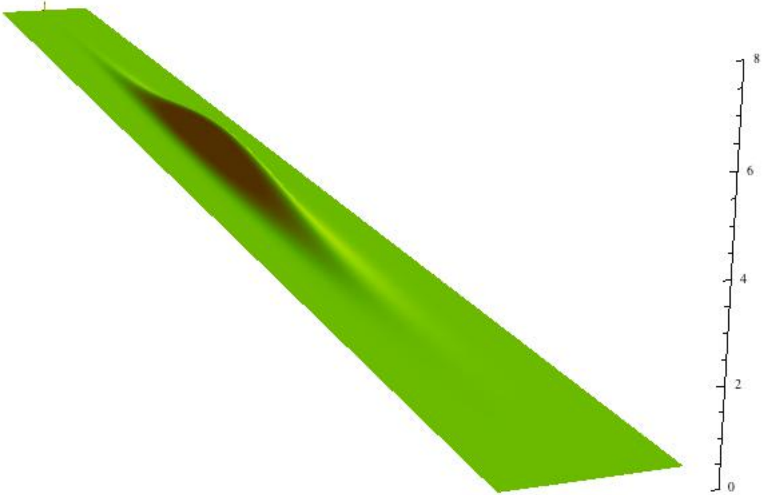

T=12,008

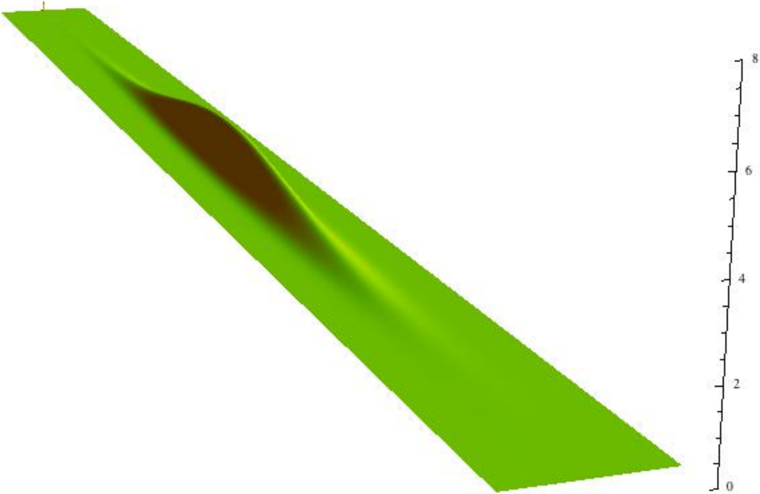

T=12,010

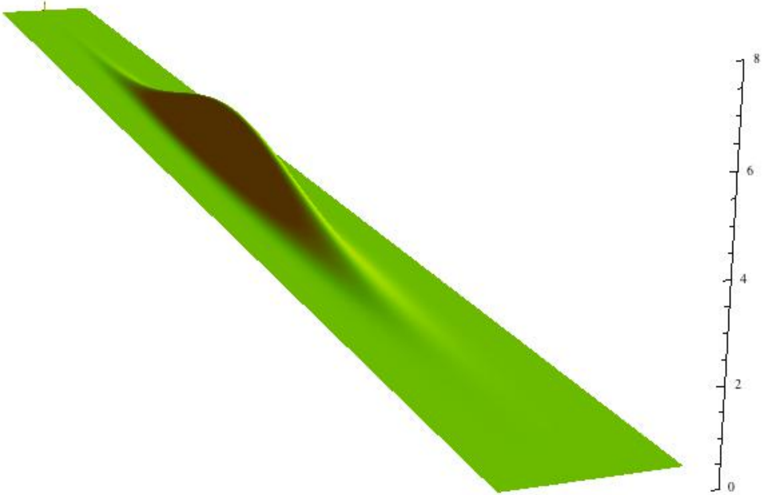

T=12,012

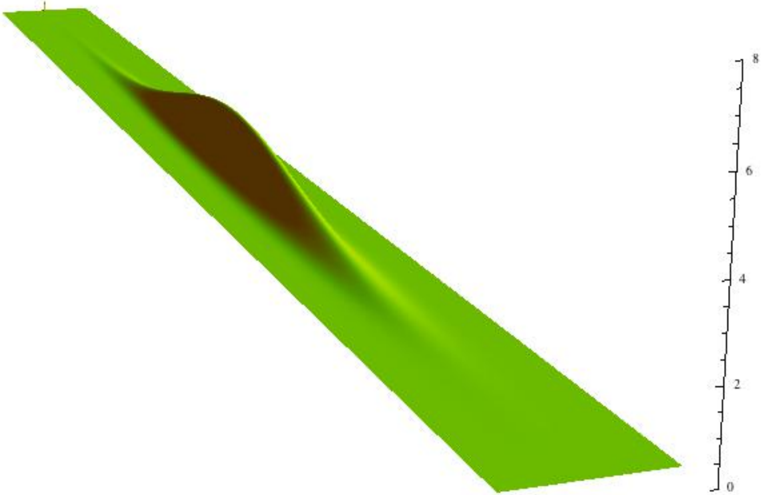

T=12,016

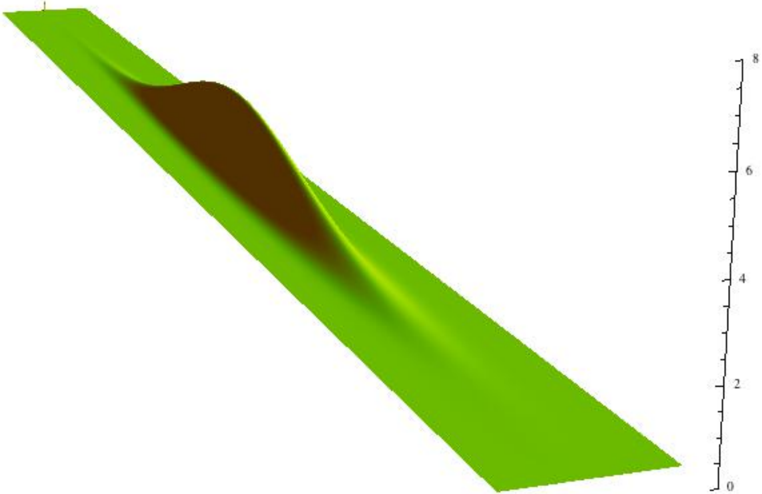

T=12,019

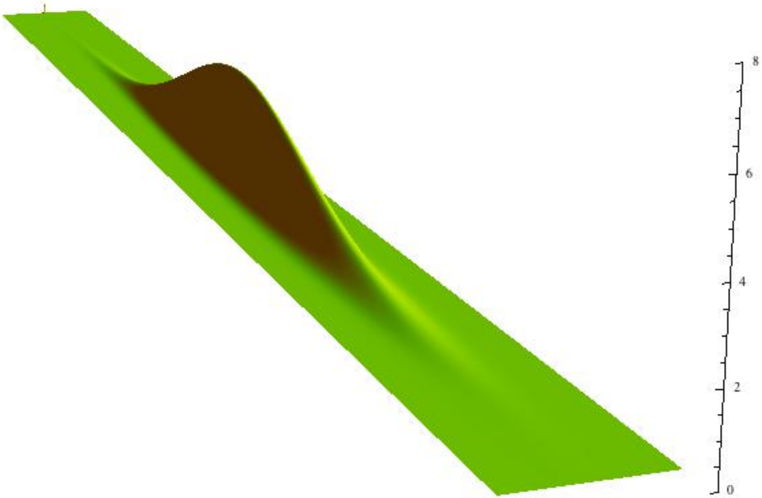

T=12,020

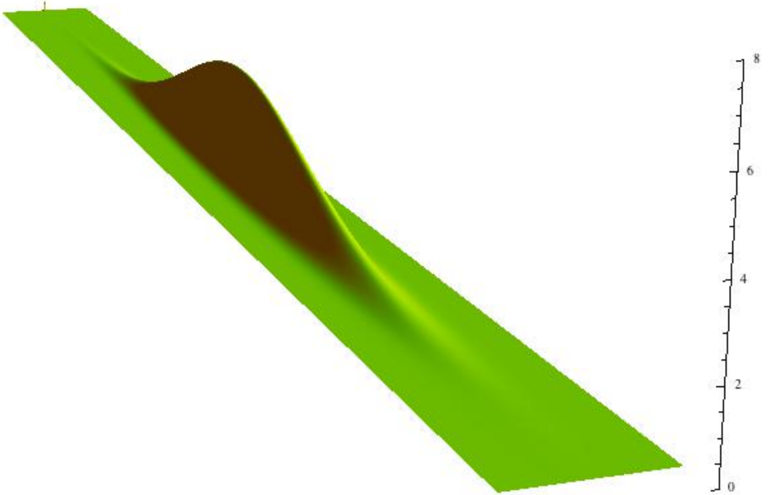

T=12,030

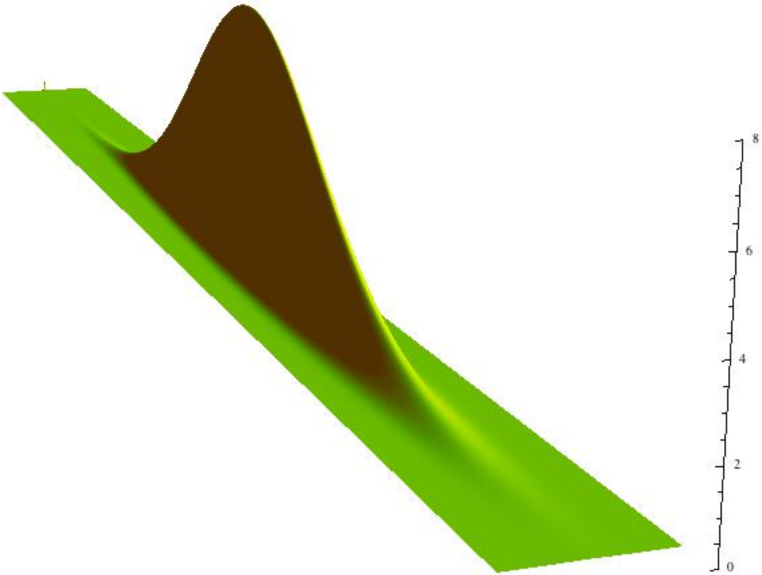

T=11,980

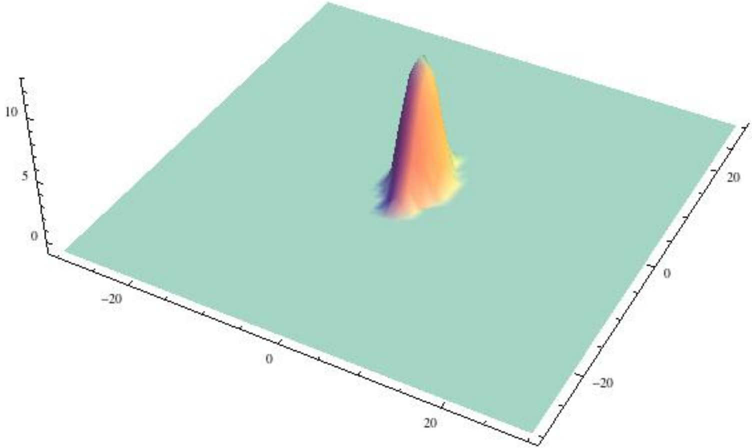

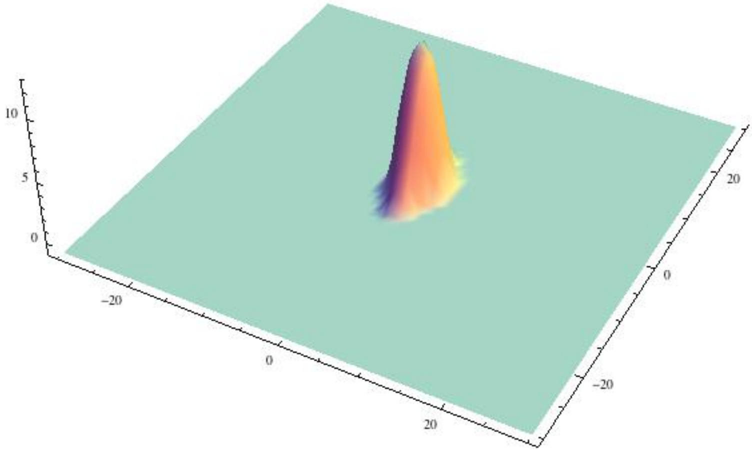
10
5
0
-20
0
20
20
0
-20

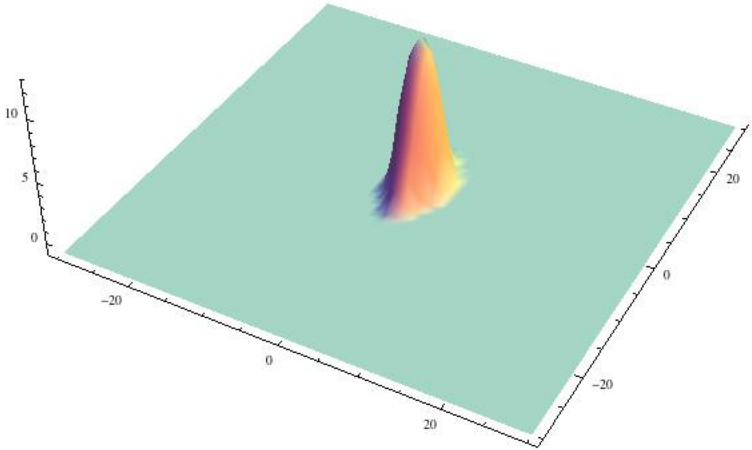
10
5
0
−20
0
20
20
0
−20

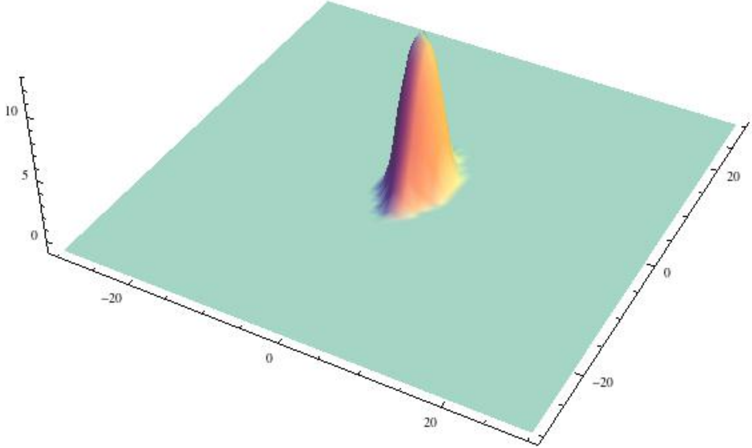
10
5
0
-20
0
20
20
0
-20

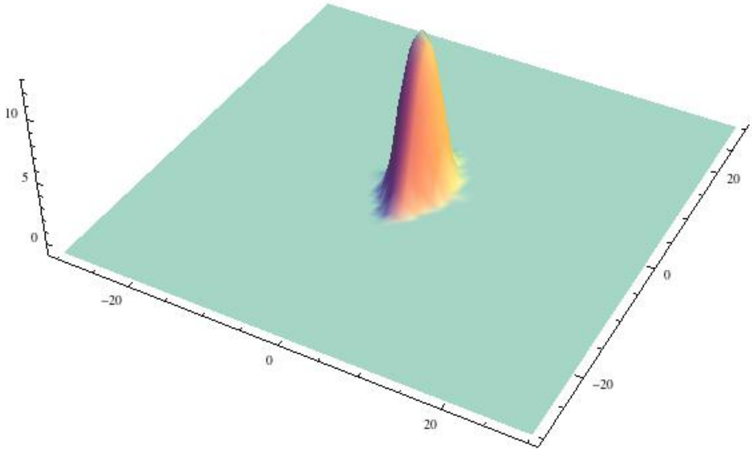

10
5
0
−20
0
20
20
0
−20

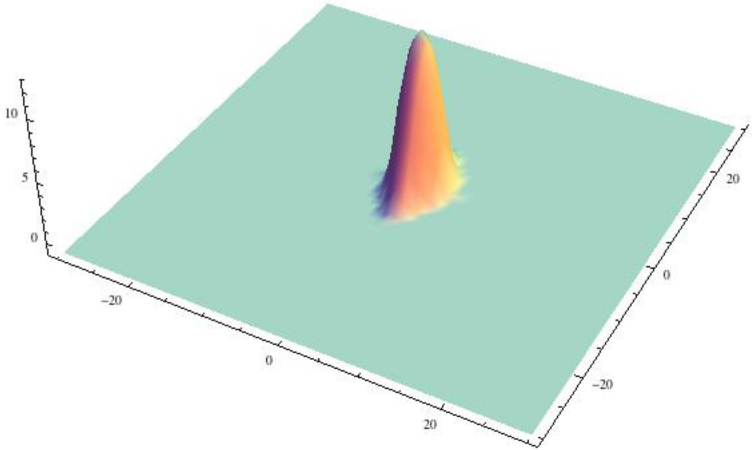
10
5
0
−20
0
20
20
0
−20

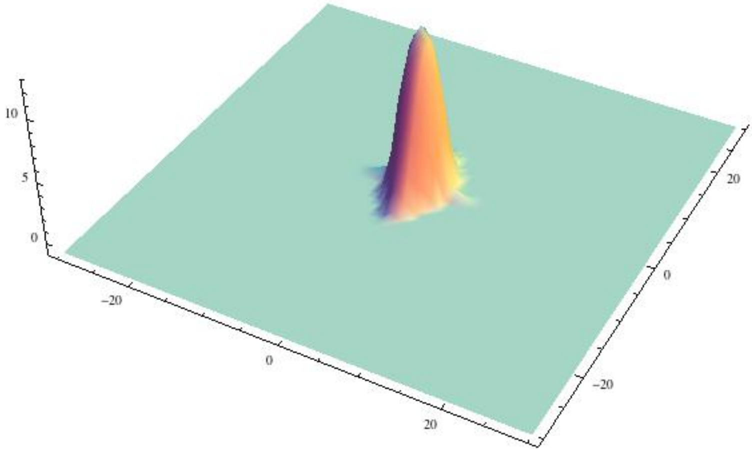
10
5
0
−20
0
20
20
0
−20

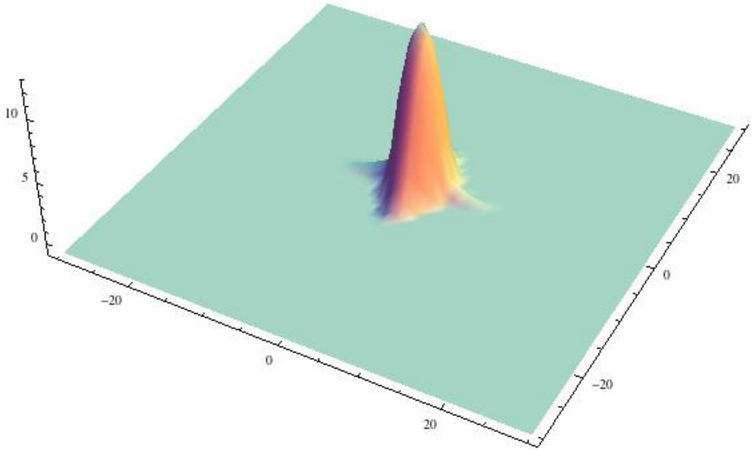

10
5
0
−20
0
20
20
0
−20

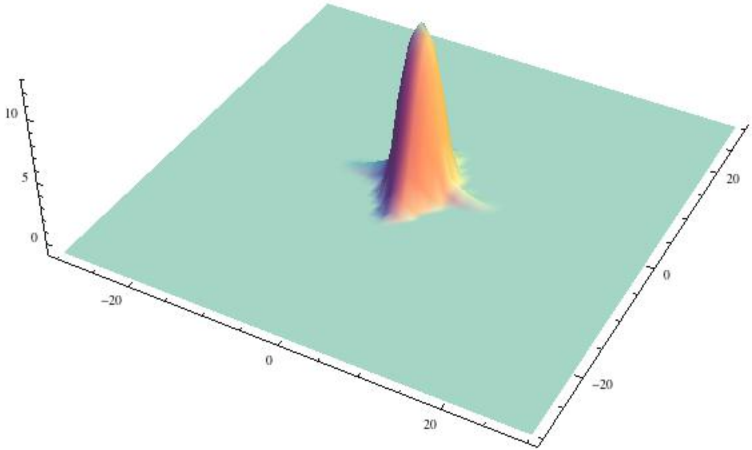
10
5
0
-20
0
20
20
0
-20

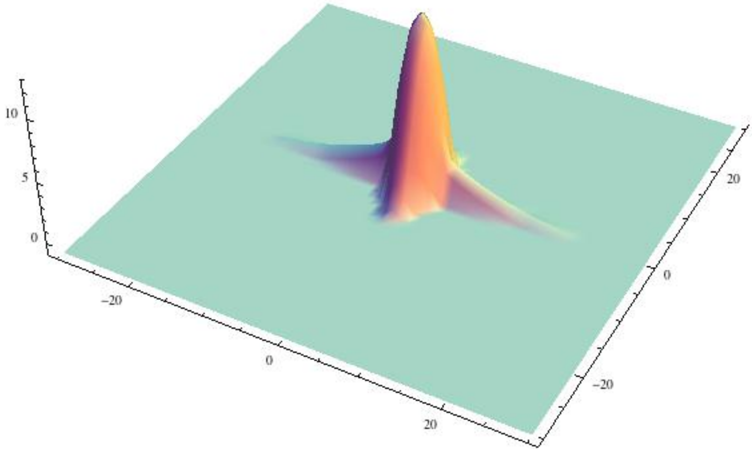
10
5
0
−20
0
20
20
0
−20

4. THE 3-d (COMPLEX) NS EQUATIONS

4. THE 3-d (COMPLEX) NS EQUATIONS

We present some preliminary results on the 3-d complex NS equations on the whole space $\mathbb{R}^3$, which in $\mathbf{k}$ space reads

$$\mathbf{v}(\mathbf{k},t) = e^{-t\mathbf{k}^2}\mathbf{v}(\mathbf{k},0) +$$

$$+\int_0^t e^{-(t-s)\mathbf{k}^2} ds \int_{\mathbb{R}^3} \langle \mathbf{v}(\mathbf{k}-\mathbf{k}',s), \mathbf{k}' \rangle \mathbf{P}_{\mathbf{k}} \mathbf{v}(\mathbf{k}',s) d\mathbf{k}'.$$

4. THE 3-d (COMPLEX) NS EQUATIONS

We present some preliminary results on the 3-d complex NS equations on the whole space $\mathbb{R}^3$, which in $\mathbf{k}$ space reads

$$\mathbf{v}(\mathbf{k},t) = e^{-t\mathbf{k}^2}\mathbf{v}(\mathbf{k},0) +$$

$$+\int_0^t e^{-(t-s)\mathbf{k}^2} ds \int_{\mathbb{R}^3} \langle \mathbf{v}(\mathbf{k}-\mathbf{k}^{'},s), \mathbf{k}^{'}\rangle \mathbf{P_k}\mathbf{v}(\mathbf{k}^{'},s) d\mathbf{k}^{'}.$$

It differs from the Burgers equations only for the orthogonal projector

$$P_{\mathbf{k}}\mathbf{v} = \mathbf{v} - \frac{\langle \mathbf{v},\mathbf{k}\rangle}{\mathbf{k}^2}\mathbf{k},$$

which expresses incompressibility.

As before, we consider real solutions which correspond to complex solutions in $\mathbf{k}$ space.

Following [Li, Sinai 2008], we again take initial data in the form of a truncated gaussian bump, centered around a point $\mathbf{k}^{(0)} = (0, 0, a)$ for some $a > 0$ large enough, and modulated by multiplying by a suitable polynomial depending on 10 parameters.

Following [Li, Sinai 2008], we again take initial data in the form of a truncated gaussian bump, centered around a point $\mathbf{k}^{(0)} = (0, 0, a)$ for some $a > 0$ large enough, and modulated by multiplying by a suitable polynomial depending on 10 parameters.

The choice of the parameters depends on the analysis of the fixed point equation.

Following [Li, Sinai 2008], we again take initial data in the form of a truncated gaussian bump, centered around a point $\mathbf{k}^{(0)} = (0, 0, a)$ for some $a > 0$ large enough, and modulated by multiplying by a suitable polynomial depending on 10 parameters.

The choice of the parameters depends on the analysis of the fixed point equation.

In [Li, Sinai 2008] it is proved that if the initial data are in an open set of such 10-parameter families of functions, the solution blows up at some finite time τ.

Following [Li, Sinai 2008], we again take initial data in the form of a truncated gaussian bump, centered around a point $\mathbf{k}^{(0)} = (0, 0, a)$ for some $a > 0$ large enough, and modulated by multiplying by a suitable polynomial depending on 10 parameters.

The choice of the parameters depends on the analysis of the fixed point equation.

In [Li, Sinai 2008] it is proved that if the initial data are in an open set of such 10-parameter families of functions, the solution blows up at some finite time τ.

Setting $\mathbf{k} = \mathbf{k}^{(0)} + \sqrt{a}\,\mathbf{Y}$ the form of the initial data looks as follows

$$v_1(\mathbf{k},0) = \frac{1}{(2\pi)^{3/2}} e^{-\frac{|\mathbf{Y}|^2}{2}} \Big(-2Y_1 + b_1^{(u)} Y_1 + b_2^{(u)} Y_1 Y_2 + b_3^{(u)} (Y_1^2 - 1) +$$

$$b_4^{(u)} Y_1 Y_3 + b_1^{(n)} Y_1 (Y_3^2 - 1) + b_2^{(n)} Y_1 Y_2 Y_3 + b_3^{(n)} (Y_1^2 - 1) Y_3 +$$

$$b_4^{(n)} Y_1 (Y_2^2 - 1) + b_5^{(n)} (Y_1^2 - 1) Y_2 + b_6^{(n)} (Y_1^3 - 3Y_1) \Big)$$

$$v_1(\mathbf{k},0) = \frac{1}{(2\pi)^{3/2}} e^{-\frac{|\mathbf{Y}|^2}{2}} \Big(-2Y_1 + b_1^{(u)} Y_1 + b_2^{(u)} Y_1 Y_2 + b_3^{(u)} (Y_1^2 - 1) +$$

$$b_4^{(u)} Y_1 Y_3 + b_1^{(n)} Y_1 (Y_3^2 - 1) + b_2^{(n)} Y_1 Y_2 Y_3 + b_3^{(n)} (Y_1^2 - 1) Y_3 +$$

$$b_4^{(n)} Y_1 (Y_2^2 - 1) + b_5^{(n)} (Y_1^2 - 1) Y_2 + b_6^{(n)} (Y_1^3 - 3Y_1) \Big)$$

$$v_2(\mathbf{k},0) = \frac{1}{(2\pi)^{3/2}} e^{-\frac{|\mathbf{Y}|^2}{2}} \Big(-2Y_2 + b_1^{(u)} Y_2 + b_2^{(u)} (Y_2^2 - 1) + b_3^{(u)} Y_1 Y_2 +$$

$$b_4^{(u)} Y_2 Y_3 + b_1^{(n)} Y_2 (Y_3^2 - 1) + b_2^{(n)} (Y_2^2 - 1) Y_3 + b_3^{(n)} Y_1 Y_2 Y_3 +$$

$$b_4^{(n)} (Y_2^3 - 3Y_3) + b_5^{(n)} Y_1 (Y_2^2 - 1) + b_6^{(n)} (Y_1^2 - 1) Y_2 \Big)$$

and the parameters b_i^u, b_j^n should be bounded by some constant.

3-d integration of the convolution is much more onerous than the 2-d integration.

3-d integration of the convolution is much more onerous than the 2-d integration.

In [Arnol'd, Kokhlov, 2009] some computational evidence of a blow-up was found, but they could not check the divergence rate of the total energy $E(t)$.

3-d integration of the convolution is much more onerous than the 2-d integration.

In [Arnol'd, Kokhlov, 2009] some computational evidence of a blow-up was found, but they could not check the divergence rate of the total energy $E(t)$.

We started a computational study of the 3-d NS equations, both complex- and real-valued, at CINECA/SCS center of Bologna and at the computer center CASPUR of the University "La Sapienza" of Rome.

3-d integration of the convolution is much more onerous than the 2-d integration.

In [Arnol'd, Kokhlov, 2009] some computational evidence of a blow-up was found, but they could not check the divergence rate of the total energy $E(t)$.

We started a computational study of the 3-d NS equations, both complex- and real-valued, at CINECA/SCS center of Bologna and at the computer center CASPUR of the University "La Sapienza" of Rome.

For complex-valued solutions we found many cases of blow-up. As for the 2-d Burgers equations we have a very stable qualitative behavior, in accordance with theoretical predictions,

3-d integration of the convolution is much more onerous than the 2-d integration.

In [Arnol'd, Kokhlov, 2009] some computational evidence of a blow-up was found, but they could not check the divergence rate of the total energy $E(t)$.

We started a computational study of the 3-d NS equations, both complex- and real-valued, at CINECA/SCS center of Bologna and at the computer center CASPUR of the University "La Sapienza" of Rome.

For complex-valued solutions we found many cases of blow-up. As for the 2-d Burgers equations we have a very stable qualitative behavior, in accordance with theoretical predictions, but we could not yet obtain enough precision in the initial state of the blow-up in order to have an estimate of the time t_c.

3-d integration of the convolution is much more onerous than the 2-d integration.

In [Arnol'd, Kokhlov, 2009] some computational evidence of a blow-up was found, but they could not check the divergence rate of the total energy $E(t)$.

We started a computational study of the 3-d NS equations, both complex- and real-valued, at CINECA/SCS center of Bologna and at the computer center CASPUR of the University "La Sapienza" of Rome.

For complex-valued solutions we found many cases of blow-up. As for the 2-d Burgers equations we have a very stable qualitative behavior, in accordance with theoretical predictions, but we could not yet obtain enough precision in the initial state of the blow-up in order to have an estimate of the time t_c.

We are now working with a refined version of FFT (”pencil” in jargon) which allows a more refined parallelization. We hope to obtain conclusive results in a short time.

We are now working with a refined version of FFT ("pencil" in jargon) which allows a more refined parallelization. We hope to obtain conclusive results in a short time.

As for the 2-d Burgers equations, the blow-up takes place in a time $\Delta \approx 10^{-5}$.

We found that if we consider initial data of the Sinai-Li type, i.e., a gaussian bump at a certain distance from the origin, all cases with energy large enough show a blow-up.

We are now working with a refined version of FFT ("pencil" in jargon) which allows a more refined parallelization. We hope to obtain conclusive results in a short time.

As for the 2-d Burgers equations, the blow-up takes place in a time $\Delta \approx 10^{-5}$.

We found that if we consider initial data of the Sinai-Li type, i.e., a gaussian bump at a certain distance from the origin, all cases with energy large enough show a blow-up.

Moreover the blow-up time decreases as the energy E grows

We are now working with a refined version of FFT ("pencil" in jargon) which allows a more refined parallelization. We hope to obtain conclusive results in a short time.

As for the 2-d Burgers equations, the blow-up takes place in a time $\Delta \approx 10^{-5}$.

We found that if we consider initial data of the Sinai-Li type, i.e., a gaussian bump at a certain distance from the origin, all cases with energy large enough show a blow-up.

Moreover the blow-up time decreases as the energy E grows and also decreases when we increase the distance a of the initial bump from the origin.

We are now working with a refined version of FFT ("pencil" in jargon) which allows a more refined parallelization. We hope to obtain conclusive results in a short time.

As for the 2-d Burgers equations, the blow-up takes place in a time $\Delta \approx 10^{-5}$.

We found that if we consider initial data of the Sinai-Li type, i.e., a gaussian bump at a certain distance from the origin, all cases with energy large enough show a blow-up.

Moreover the blow-up time decreases as the energy E grows and also decreases when we increase the distance a of the initial bump from the origin.

Behavior of the energy near the critical time for a typical case ($a = 5$, on a space mesh of $100 \times 100 \times 200$ points):

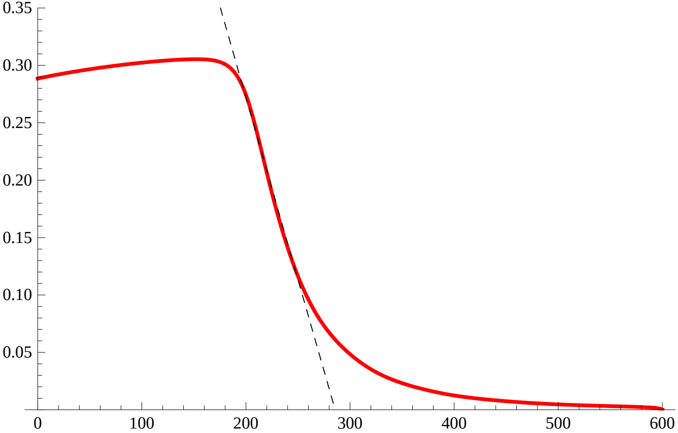

Figure: $(E(t))^{-1/5}$ *versus* $t \cdot 10^5$ *for* $\delta_t = 10^{-5}$, $\delta_{\mathbf{k}} = \{1, 1, 1\}$, $b_i^u = b_j^n = 0 \ \forall i, j$, $E(0) = 500$.

We also started a preliminary study of the real solutions of the 3-d NS equations associated to the exploding complex solutions, We also started a preliminary study of the real solutions of the 3-d NS equations associated to the exploding complex solutions, which are obtained by (anti)symmetrizing the initial conditions of Li-Sinai type.

The computer simulations show that the solutions behave for some time as real solutions, satisfying the energy inequality

$$E(t) + \frac{\nu}{2} \int_0^t En(s) ds \leq E(0)$$

where $En(t)$ is the enstrophy

$$En(t) = \frac{1}{2} \int_{\mathbb{R}^3} \mathbf{k} |\mathbf{k}|^2 |\mathbf{v}(\mathbf{k}, t)|^2.$$

But after some time, due to the round-off error, it loses symmetry and starts exploding as the one-bump complex solution.

WITH ALL BEST WISHES
TO ANDRAS

LERAY, J. 1934 Sur le mouvement d'un liquide visqueux emplissant l'éspace. *Acta Math.* **63**, 193–248.

LI, D.& SINAI, YA. G. 2008 Blowups of complex solutions of the 3D Navier-Stokes system and renormalization group method. *J. Eur. Math. Soc.* **10**, 267–313.

LI, D.& SINAI, YA. G. 2010 Singularities of complex-valued solutions of the two-dimensional Burgers system. *J. Math. Phys.* **51**, 01525.

ARNOL'D, M. D. & KHOKHLOV, A. V. 2009 Modeling a blow-up solution of tornado type for the complex version of the three dimensional Navier-Stokes equation. *Russian Mathematical Surveys.* **64**, 1133–1135.

BOLDRIGHINI, C., FRIGIO, S., & MAPONI, P. 2012 Exploding solutions of the complex two-dimensional Burgers equations: computer simulations. *J. Math. Phys.* **53** 083101.

$$\|\phi\|^2 = \frac{1}{2\pi\sigma^2} \int_{\mathbb{R}^2} |\phi(\mathbf{k})|^2 e^{-\frac{\mathbf{k}^2}{2\sigma^2}} \, d^2\mathbf{k} \tag{3}$$

$$\mathbf{w}^{(A)}(\mathbf{k},t) = A\, e^{-t\mathbf{k}^2}\mathbf{w}^{(1)}(\mathbf{k}) +$$

$$+\int_0^t e^{-\mathbf{k}^2(t-s)} \sum_{p=2}^{\infty} A^p g^{(p)}(\mathbf{k},s)ds. \tag{4}$$

$$\mathbf{g}^{(p)}(\mathbf{k},t)=\int_0^t ds_2\cdot$$

$$\cdot\int_{\mathbb{R}^2}\langle\mathbf{w}^{(1)}(k-k^{'},s),\mathbf{k}^{'}\rangle\mathbf{g}^{(p-1)}(\mathbf{k}^{'},s)e^{-t(\mathbf{k}-\mathbf{k}^{'})^2-t(\mathbf{k}^{'})^2}d\mathbf{k}^{'},+$$

$$+\sum_{\substack{p_1+p_2=p\\ p_1,p_2>1}}\int_0^t ds_1\int_0^t ds_2\cdot \tag{5}$$

$$\cdot\int_{\mathbb{R}^2}\langle\mathbf{g}^{(p_1)}(\mathbf{k}-\mathbf{k}^{'},s_1),\mathbf{k}^{'}\rangle\mathbf{g}^{(p_2)}(\mathbf{k}^{'},s_2)e^{-(t-s_1)(\mathbf{k}-\mathbf{k}^{'})^2-(t-s_2)(\mathbf{k}^{'})^2}d\mathbf{k}^{'}+$$

$$+\int_0^t ds_1\int_{\mathbb{R}^2}\langle\mathbf{g}^{(p-1)}(\mathbf{k}-\mathbf{k}^{'},s_1),\mathbf{k}^{'}\rangle\mathbf{w}_1(\mathbf{k}^{'})e^{-(t-s_1)(\mathbf{k}-\mathbf{k}^{'})^2-t(\mathbf{k}^{'})^2}d\mathbf{k}^{'}$$

$$\mathbf{h}^{(p)}(\mathbf{Y},t) = \frac{p^2}{4a^2}\cdot \tag{7}$$

$$\cdot \sum_{\substack{p_1+p_2=p\\ p_1,p_2>1}} \frac{1}{p_1^2 p_2^2} \int_{\mathbb{R}^2} \frac{p_2}{p} \sum_{j=1}^{2} h_j^{(p_1)}\left(\frac{\mathbf{Y}-\mathbf{Y}'}{\sqrt{\gamma}}, t\right) \mathbf{h}^{(p_2)}\left(\frac{\mathbf{Y}'}{\sqrt{1-\gamma}}, t\right) d\mathbf{Y}'.$$

$$\mathbf{h}^{(r)}(\mathbf{Y},t) = r\, Z(t)(\Lambda_p(t))^r \frac{e^{-\frac{\mathbf{Y}^2}{2\sigma^2}}}{2\pi\sigma^2} \left(\mathbf{H}(\mathbf{Y}) + \delta_r(\mathbf{Y},t)\right), \qquad (8)$$

$$\mathbf{h}^{(r)}(\mathbf{Y},t) = r\, Z(t)(\Lambda_p(t))^r \frac{e^{-\frac{\mathbf{Y}^2}{2\sigma^2}}}{2\pi\sigma^2} \left(\mathbf{H}(\mathbf{Y}) + \delta_r(\mathbf{Y},t)\right), \qquad (8)$$

$$\mathbf{H}(\mathbf{Y})\frac{e^{-\frac{\mathbf{Y}^2}{2\sigma^2}}}{2\pi\sigma^2} = \int_0^1 d\gamma(1-\gamma)\int_{\mathbb{R}^2} d\mathbf{Y}'\mathbf{H}\left(\frac{\mathbf{Y}'}{\sqrt{1-\gamma}}\right)\cdot \tag{9}$$

$$\cdot \left[H_1\left(\frac{\mathbf{Y}-\mathbf{Y}'}{\sqrt{\gamma}}\right)+H_2\left(\frac{\mathbf{Y}-\mathbf{Y}'}{\sqrt{\gamma}}\right)\right]\frac{e^{-\frac{(\mathbf{Y}-\mathbf{Y}')^2}{2\sigma^2\gamma}}}{2\pi\sigma^2\gamma}\frac{e^{-\frac{(\mathbf{Y}')^2}{2\sigma^2(1-\gamma)}}}{2\pi\sigma^2(1-\gamma)}.$$

$$\sum_p A^p \mathbf{g}^{(p)}(\mathbf{k},t) \approx C \sum_p p \left(\frac{\Lambda(t)}{\Lambda(\tau)}\right)^p \frac{e^{-\frac{(\mathbf{k}-p\mathbf{k}^{(0)})^2}{2ap\sigma^2}}}{2\pi\sigma^2} \mathbf{H}_0(\mathbf{Y}), \qquad (10).$$

$$\sum_p A^p \mathbf{g}^{(p)}(\mathbf{k}, t) \approx C \sum_p p \left(\frac{\Lambda(t)}{\Lambda(\tau)} \right)^p \frac{e^{-\frac{(\mathbf{k} - p\mathbf{k}^{(0)})^2}{2ap\sigma^2}}}{2\pi\sigma^2} \mathbf{H}_0(\mathbf{Y}), \qquad (10).$$